Available online at www.sciencedirect.com
SCIENCE DIRECT
Journal of Computational Physics 215 (2006) 717–740
JOURNAL OF COMPUTATIONAL PHYSICS
www.elsevier.com/locate/jcp

Asymptotic preserving and positive schemes for radiation hydrodynamics

Christophe Buet *, Bruno Despres

Département des Sciences de la Simulation et de l'Information, Commissariat à l'Énergie Atomique, 91680, Bruyères le Chatel, BP 12, France

Received 16 March 2005; received in revised form 5 November 2005; accepted 9 November 2005
Available online 4 January 2006

Abstract

In view of radiation hydrodynamics computations, we propose an implicit and positive numerical scheme that captures the diffusion limit of the two-moments approximate model for the radiative transfer even on coarses grids. The positivity of the scheme is equivalent to say that the scheme preserves the limited flux property. Various test cases show the accuracy and robustness of the scheme.

Keywords: Radiation hydrodynamics; Diffusion limit; Flux limited; Monotone scheme

1. Introduction

The aim of this work is about accurate discretization of radiation hydrodynamics by means of eulerian finite volume methods. In this direction we study and discretize a non-linear two-moments model (2) for radiation in the Eulerian frame written in one space dimension. The model, called in the next M^1, derives from a maximum entropy principle as in [10,27,19,26,5,1]. This model and the related ones are stiff models, the stiffness parameter is ε small. For ICF (inertial confinement fusion applications) $\varepsilon \approx 10^{-3}$, for example see [30]. There are some regions of the space with very little interactions between the radiation and the matter and other regions with strong interactions with the matter. The case of little interactions is called the streaming regime. For strong interaction it is possible to derive diffusion approximations of (2). This is called the diffusion regime. Among the numerical methods that have been proposed for the discretization of simplified radiation models, we distinguish between discretization of diffusion approximations and direct discretization of two-moment models. Concerning numerical method for the discretization of diffusion approximations we quote [18] in which a technique of flux limiting is discussed in detail. The technique of flux limiting somehow extends the domain of validity of these diffusion approximations to the streaming regime. We exhibit a new intermediate interaction regime, of pure hyperbolic type, for which the limit

* Corresponding author.
E-mail addresses: christophe.buet@cea.fr (C. Buet), bruno.despres@cea.r (B. Despres).

0021-9991/$ - see front matter © 2005 Elsevier Inc. All rights reserved.
doi:10.1016/j.jcp.2005.11.011

equation can be written in divergent form or in non-divergent form. We privilege the divergence form of this equation. This is different from the work of [9] where the non-divergent formulation is used for the radiation energy. This is important for the numerics since a non-divergent discretization may converge to wrong discontinuous solutions [17]. It has been noticed since a long time, in the work of Mihalas [24] for example, that a direct discretization of a two-moments models can help to get a better discretization for both streaming and diffusion regimes. It is also possible that higher moments models could treat more efficiently the anisotropy of radiation in dimension greater than one.

In this direction, a preliminary question is how to discretize "correctly" a two-moments model for the radiation in the non-relativistic case in dimension one, that is for ε small, and at the matter scale. That is, we desire to adapt the grid according to the length scale of the matter. From the point of view of photons the grid is coarse. Among the works dedicated to this specific problem we point out [21–23,2]. We show on a simple example that freezing naively the Eddington factor during the time step gives a non-positive implicit linear discretization of the problem. This is based on the fact that the linear implicitation of the HLL solver is non-positive if the equation is non-linear, that is if the Eddington factor is not constant. The new method we propose has the following features:

Positivity of the scheme: the scheme guarantees the positivity in 1D

$$-E_r \leqslant F_r \leqslant E_r$$

where E_r is the energy of radiation and F_r is the radiation flux. This is equivalent to say the scheme is *flux limited*

$$\frac{|F_r|}{E_r} \leqslant 1. \tag{1}$$

The physical meaning of flux limitation is more natural with (1). This property is useful essentially in the streaming regime for which $|F_r| \approx E_r$. This flux limiting has nothing to do with the numerical tricks used for the discretization of diffusion approximations of two-moments models.

Correct diffusion limits: the equilibrium and non-equilibrium diffusion limits of the scheme are correct even for a coarse mesh,

Correct hyperbolic limit: the numerical treatment of the purely hyperbolic limit (9) is compatible with the divergent form of the equation.

Time step requirement: the scheme is explicit for the hydrodynamic part and totally implicit for the radiation part. Therefore, the only CFL limitation comes from the hydrodynamic part.

The first three properties are true at the PDE level for the basic two-moments model. Since the basic two-moments model considered in this paper is highly non-linear (see (2)), a direct implicit discretization of this model may be tricky if the material velocity v is non-zero. We now describe the strategy we propose to obtain these properties at the numerical level. We think this approach is simpler.

The first ingredient to obtain all these properties is what we call a splitted approximation. Usually this kind of model is called a co-moving frame radiation hydrodynamics model, see [25,20,2]. The model consists in transporting the radiation entropy and the radiation entropy flux at velocity v, then to discretize with the matter at rest with $v = 0$. This splitted approximation has almost zero additional numerical cost. The maximal hyperbolic wave velocity of the splitted approximation is $\frac{1}{\varepsilon} \pm v$ which slightly exceeds the physical maximal wave velocity $\frac{1}{\varepsilon}$ which is the velocity of light in non-dimensional variables. This is shared with other co-moving frame radiation hydrodynamics model like [25,20,2]. We think that slight violation of the velocity of light in very rare cases is much better than diffusion approximations without flux limiting of the diffusion coefficient. Even with flux limiting of the diffusion coefficient it is difficult to guarantee a correct velocity for the front propagation in transparent materials. In this work we only consider an explicit discretization of the hydrodynamics part. On the other hand, the radiative step of the splitted model is discretized by an implicit method. The reason is the high speed of the radiation signal which is much greater than the mean velocity of the matter. Since we are interested in the time scale of the matter, the radiation must be treated implicitly.

The second ingredient lies in the discretization of the radiative step. The numerical scheme for the radiative step must be consistent with the diffusion approximation in opaque region and must preserve the flux limited property. It is well known, cf. [14,15,28], that in opaque regions standard finite volume schemes lead to a wrong coefficient of diffusion for coarse grids. It is illuminating to consider the hyperbolic heat equation

$$\partial_t u + \frac{1}{\varepsilon}\partial_x v = 0, \quad \partial_t u + \frac{1}{\varepsilon}\partial_x v = -\frac{1}{\varepsilon^2}u.$$

The asymptotic regime $\varepsilon \to 0^+$ is the heat equation $\partial_t u - \partial_{xx} u = 0$. The problem stressed in [14,15,28] is that a discretization with stable upwinded schemes of the hyperbolic equation has the asymptotic limit

$$\partial_t u - \left(1 + \frac{C\Delta x}{\varepsilon}\right)\partial_{xx} u = 0, \quad C > 0.$$

Therefore, the discretization of the hyperbolic equation on a coarse grid may have the limit

$$\partial_{xx} u = 0$$

which is wrong. Last decade "asymptotic preserving schemes" (AP scheme), cf. [14,15,28,12], have been developed in order to recover the correct diffusion asymptotic limit. Thus AP schemes seems to be the good tool for radiative two-moment models. But actual AP schemes suffer of some limitations. Semi-implicit AP scheme like those proposed in [15,14] can handle non-linear system but are, in the best case, only positive and stable under a parabolic CFL condition and this not acceptable for our purpose since we do not want such time step limitation. The AP scheme proposed by Gosse in [12] has a better stability property, but it is difficult to extend this scheme for non-linear systems: Moreover, the method used in [12] seems quite impossible to extend for a resonant problem like the one we study in this work. Therefore, we have developed a new discretization of radiation part of the model. This implicit discretization is unconditionally positive, and has the correct diffusion limit. It is based on two basic schemes. The first one is a "relaxation" scheme, see for example [16], which has the advantage to transform the initial non-linear problem into a linear one: this is why we solve two linear systems at each time step. The second one is the AP scheme described [12], in order to obtain the right asymptotic diffusion limit with no time step limitation for the positivity. This discretization of the radiative step is an improved version of the one proposed in [7], it can handle more efficiently opaque and transparent zones. Concerning the cost of such a discretization, let us mention that in one dimension the matrix can be inverted by the a low cost algorithm like the LU one.

The plan is as follows. In Section 2, we study the M^1 model for the radiation and recall various diffusion approximations of this model. In Section 3, we derive what we call splitted approximations for the M^1 model. Numerical schemes for each part of the splitting are proposed and analyzed in Section 4. In Section 5, we show some numerical results to demonstrate the features of the scheme, with application to the full system of hydrodynamics coupled with radiation. Section 6 is the conclusion. We sketch future developments of the method.

2. Basic equations

2.1. The two-moments model M^1

The starting point of the analysis is the following two-moments model for radiation in the Eulerian frame and written with non-dimensional variables in one space dimension (see [1] for a full derivation)

$$\begin{aligned}
&\frac{\partial}{\partial t}E_r + \frac{1}{\varepsilon}\frac{\partial}{\partial x}F_r = \frac{\gamma\sigma_a}{\varepsilon^2}(T^4 - E_r + \varepsilon v F_r) - \frac{\gamma\sigma_s}{\varepsilon}vF_r^0,\\
&\frac{\partial}{\partial t}F_r + \frac{1}{\varepsilon}\frac{\partial}{\partial x}P_r = -\frac{\gamma\sigma_a}{\varepsilon^2}(F_r - \varepsilon v(T^4 + P_r)) - \frac{\gamma\sigma_s}{\varepsilon^2}F_r^0,\\
&P_r = \chi E_r, \quad \chi = \frac{3+4f^2}{5+2\sqrt{4-3f^2}}, \quad f = F_r/E_r.
\end{aligned} \tag{2}$$

In this model E_r is the energy of radiation, F_r is the flux of radiation, P_r is the pressure of radiation and χ is called the Eddington factor. f measures the anisotropy of radiation. For physical reasons the modulus of f is

bounded by one, $|f| \leqslant 1$. This Eddington factor was proposed first by Levermore [18] and can be recovered from a maximum entropy principle as in [27,19,26,5]. For a matter at rest, it can be checked, by means of the Godunov method, that solutions of the system (2) for a general Eddington factor χ verify this flux limited property provided a) the initial condition satisfies it, b) the Eddington factor χ is a even convex positive function satisfying $\chi(\pm 1) = 1$. The Eddington factor considered here has these properties.[1]

This system has two exterior parameters. The first one is T the temperature of the matter. ε is a small parameter that measures the velocity of light versus the sound velocity in the matter. For non-relativistic plasmas the velocity of the matter can be assumed of the same magnitude than sound velocity in the matter, therefore is also small with respect to the velocity of light. The second exterior parameter is v the velocity of the matter. Therefore, $\gamma = 1/\sqrt{1-\varepsilon^2|v|^2} \geqslant 1$ is very close to one for non-relativistic plasmas. F_r^0 is the radiation flux energy measured in the co-mobile reference frame that moves with the matter $F_r^0 = \gamma^2((1+\varepsilon^2 v^2)F_r - \varepsilon v(E_r + P_r))$. The particular form of the right-hand side is due to the underlying compatibility of the relaxation source terms with the Lorentzian invariance of radiation. The absorption–emission opacity σ_a and the scattering opacity σ_s are mean opacities. In practice there are functions of T and the density of the matter. This model, (2), comes from a maximum entropy principle with Lorentzian invariant source terms [1]. In particular, one can take $\gamma = 1$ in (2). Other simpler sources have been proposed in the literature [20]. The conclusions of the present study are easy to generalize to the source terms of [20] which are very close to the ones used in this work.

2.2. Hyperbolicity and entropy of the radiation

The M^1 model (2) is strictly hyperbolic for $0 \leqslant f^2 < 1$ and $1 < f^2 < \frac{4}{3}$. For $f^2 = \frac{4}{3}$ it is non-more differentiable. For $f = 1$ the Jacobian matrix of the flux is $\frac{\partial(F_r,P_r)}{\partial(E_r,F_r)} = \left(\begin{smallmatrix} 0 & 1 \\ 0 & 2 \end{smallmatrix}\right)$. Therefore, the system is only weakly hyperbolic at $f = \pm 1$. We notice that $f = \pm 1$ corresponds to a strongly non-isotropic radiation flux. Since the eigenvalues coincide for $f = \pm 1$ it means the system is resonant for $|F_r| = E_r$.

The method of moment assumes the intensity of the radiation is the generalized Planckian $\frac{4\pi^5 I}{15\, v^3} = \frac{1}{e^{\frac{v}{T_r} + \frac{vbn}{T_r}} - 1}$. The energy of radiation and the radiation flux can also be computed with respect to T_r and b. One has $E_r = \int\int I(v,n)\,\mathrm{d}v\,\mathrm{d}n$, $F_r = \int\int nI(v,n)\,\mathrm{d}v\,\mathrm{d}n$ and $P_r = \int\int n \otimes nI(v,n)\,\mathrm{d}v\,\mathrm{d}n$. After some standard calculations [27,1] one gets

$$E_r = T_r^4 \frac{3+b^2}{3(1-b^2)^3}, \quad F_r = -T_r^4 \frac{4b}{3(1-b^2)^3}. \tag{3}$$

Let S_r and Q_r be the entropy and entropy flux of the radiation defined by $S_r = -\frac{15}{4\pi^5}\int\int v^2(n\log n - (n+1)\log(n+1))\,\mathrm{d}v\,\mathrm{d}n$ and $Q_r = -\frac{15}{4\pi^5}\int\int v^2(n\log n - (n+1)\log(n+1))n\,\mathrm{d}v\,\mathrm{d}n$. One gets the simplified expressions

$$S_r = \frac{4}{3}\frac{T_r^3}{(1-|b|^2)^2}, \quad Q_r = -bS_r. \tag{4}$$

The mapping $(E_r, F_r) \mapsto (T_r, b)$ is degenerate for $b = \pm 1$. Since $\frac{F_r}{E_r} = f = -\frac{4b}{3+b^2}$, then $b = \pm 1$ is equivalent to $f = \mp 1$. It has been proved in [1] (anyway this is compatible with the theory of moment for hyperbolic system of conservation laws, see [18]) that an algebraic combination of the two equations of the system (2) gives the equation $\frac{\partial}{\partial t}S_r + \frac{1}{\varepsilon}\frac{\partial}{\partial x}Q_r = \frac{1}{T_r}S_E + \frac{b}{T_r}S_F$. This comes from the second principle of thermodynamic for the moment model, namely $T_r\,\mathrm{d}S_r = \mathrm{d}E_r + b\,\mathrm{d}F_r$.

2.3. Equilibrium diffusion limit

Very classically [20,21] the equilibrium diffusion limit of (2) is recovered with the scaling $\sigma_a = \mathrm{O}(1)$ and $\sigma_s = \mathrm{O}(1)$. Then of course the dominant contribution in the right-hand side of (2) is due to σ_a. One gets

[1] A particular approximation of (2) is called the P^1 model, for which the Eddington factor is a constant function $\chi = 1/3$. This value comes from the choice $f = 0$ in (2). Since the P^1 model is linear, it is trivial to check that the solutions of this model do not verify the flux limited property.

$E_r = T^4 + O(\varepsilon)$, $F_r = -\varepsilon \frac{1}{\sigma_a+\sigma_s}\partial_x P_r + \varepsilon \frac{4}{3} T^4 + O(\varepsilon^2)$ and $P_r = \frac{1}{3}T^4 + O(\varepsilon)$. Since $F_r = O(\varepsilon)$ then $\chi \approx \frac{1}{3}$. Assuming $v = 0$ a typical diffusion equilibrium model for the temperature is [20]

$$\frac{\partial}{\partial t}(T + T^4) = \partial_x \left(\frac{1}{3(\sigma_a + \sigma_s)} \partial_x T^4 \right). \tag{5}$$

This type of model is valid only in opaque materials, but is also used outside of its natural validity domain in transparent materials for which σ_a and σ_s are very small. To see what is the problem in transparent materials it is sufficient to notice that the model is degenerate parabolic and admits finite speed of propagation for the fronts $T = 0$. At the front the temperature can be expanded like $T \approx C_1 |x - x_f(t)|^{\frac{1}{3}}$. The speed of propagation of the front is $x_f'(t) = \frac{C_2}{3(\sigma_a+\sigma_s)} \partial_x T^3$. Provided $\partial_x T^3 = O(1)$ the propagation of the front is highly non-physical in transparent materials since the $|x_f'(t)| \to \infty$. In any cases $|x_f'(t)|$ should be smaller than $\frac{1}{\varepsilon}$.

2.4. Non-equilibrium diffusion limit

It has recently been noticed that the scaling $\sigma_a = O(\varepsilon)$ and $\sigma_s = O(1)$ helps to get a non-equilibrium diffusion limit of the M^1 model. Here non-equilibrium means that $E_r \neq T^4$. It explains why σ_a needs to be small. On the other hand, σ_s is kept of order one, so that the M^1 model admits a diffusion limit. Thus the model we presents hereafter is a simple non-trivial model for the coupling of radiation and hydrodynamics. With the above scaling one gets $E_r = T_r^4 + O(\varepsilon)$, $F_r = -\varepsilon \frac{1}{\sigma_s}\partial_x T_r^4 + \varepsilon \frac{4}{3} v T_r^4 + O(\varepsilon^2)$ and $P_r = \frac{1}{3} T_r^4 + O(\varepsilon)$. With these asymptotics and definitions, then the equation for E_r becomes

$$\frac{\partial}{\partial t} E_r + \frac{\partial}{\partial x}\left(-\frac{1}{\sigma_s}\frac{\partial}{\partial x} E_r + \frac{4}{3} v E_r \right) = \sigma_a (T^4 - E_r) + v \frac{\partial}{\partial x}\left(\frac{1}{3} E_r \right). \tag{6}$$

One gets

$$\frac{\partial}{\partial t} E_r + \frac{\partial}{\partial x}(v E_r) + \frac{E_r}{3}\frac{\partial}{\partial x} v = \sigma_a (T^4 - E_r) + \frac{\partial}{\partial x}\left(\frac{1}{\sigma_s}\frac{\partial}{\partial x} E_r \right). \tag{7}$$

Thus the radiation energy E_r is the solution of a fluid like equation with pressure $P_r = \frac{1}{3}E_r$. In (7) the velocity is a given function of time and space $v = v(t,x)$: $\frac{\partial}{\partial x} v \neq 0$ a priori. Therefore, v may be discontinuous. Other approximations of the two-moments model exist in the literature. One commonly used consists in using (7) with another definition of the radiative pressure and with $\sigma_t = \sigma_a + \sigma_s$ in the right-hand side. One gets

$$\frac{\partial}{\partial t} E_r + \frac{\partial}{\partial x}(v E_r) + \frac{E_r}{3}\frac{\partial}{\partial x} v = \sigma_a (T^4 - E_r) + \frac{\partial}{\partial x}\left(\frac{1}{\sigma_a + \sigma_s}\frac{\partial}{\partial x} E_r \right). \tag{8}$$

It means that σ_a is no more considered as a very small quantity with respect to σ_s. We will use this model in the numerical section. The interest of such models is clear. Paraphrasing [25]: The radiation temperature T_r can be quite different from the material temperature. The spectrum of the radiation field can be non-Planckian.

The model (8) has the same limitation than equilibrium diffusion approximation like (5) in transparent materials, that is σ_a and σ_s small. However, a new intermediate regime appears. Let us assume that σ_a is small and σ_s large. For example $\sigma_a = O(\varepsilon)$ and $\sigma_s = O(\varepsilon^{-1})$. In this case the equation becomes

$$\frac{\partial}{\partial t} E_r^{\frac{3}{4}} + \frac{\partial}{\partial x} v E_r^{\frac{3}{4}} = 0 \iff \frac{\partial}{\partial t} E_r + \frac{\partial}{\partial x} v E_r + \frac{E_r}{3}\frac{\partial}{\partial x} v = 0. \tag{9}$$

The equation is written in divergence form on the left and in non-divergence form on the right. The $\frac{E_r}{3}$ term in the non-divergence form is the thermodynamic pressure of radiation [25]. The divergence form of the equation if a conservation equation for $E_r^{\frac{3}{4}}$ which is the number of photons at equilibrium. Assuming the matter encounters a shock, the velocity v is the discontinuous. Therefore, a continuous radiation energy E_r is required to give a non-ambiguous value to the non-conservative product $\frac{E_r}{3}\frac{\partial}{\partial x} v$. Unfortunately, the hypothesis $\sigma_s = O(\varepsilon^{-1})$ implies a vanishing diffusion and possible discontinuity of E_r at the limit. So the non-conservative product $\frac{E_r}{3}\frac{\partial}{\partial x} v$ can be ambiguous. On the other hand, the divergence form of the equation is non-ambiguously defined for a discontinuous velocity. The Rankine Hugoniot relations for the divergence formulation of (9) are

$$-D[T_r^3] + [vT_r^3] = 0, \quad E_r = T_r^4.$$

D is the shock velocity. Assuming radiation is at equilibrium the radiation entropy is $S_r = T_r^3$ and is also equal to the number of photons. Therefore, the physical meaning of this RH relation is that the integrated number of photons $\int T_r^3$ is conserved through the discontinuity. This is compatible with what is proposed at the numerical level in [25], where no numerical viscosity is used for radiation. The situation is very closed to ion-electron fluid models, for which the correct Rankine Hugoniot relation is obtained with the entropy of electron, see [35,8]. There is no entropy deposit on electrons or photons at shocks. This principle is compatible with the conservation of total energy, the total energy being the sum of the radiation energy and the fluid energy. For contact discontinuities $D = v_L = v_R$ the Rankine Hugoniot relation vanishes.

2.5. Splitting method for the non-equilibrium diffusion limit

We begin with a preliminary remark about the discretization in time of the non-equilibrium diffusion limit equation (7). The idea is to solve (7) with a splitting technique, that is we solve separately during the same time step

$$\partial_t S_r + \partial_x v S_r = 0, \quad S_r = \frac{4}{3} T_r^3 \text{ followed by } \partial_t E_r = \sigma_a (T^4 - E_r) + \frac{\partial}{\partial x}\left(\frac{1}{3\sigma_t}\frac{\partial}{\partial x} E_r\right), \quad E_r = T_r^4. \tag{10}$$

The first equation in (10) is, for smooth solutions, algebraically equivalent to $\partial_t E_r + \partial_x v E_r + \frac{1}{3} T_r^4 \partial_x v = 0$. Therefore, (10) is indeed a convenient way to split (7) into two separate parts. Note that the first equation in (10) is a first order conservation law, that can be easily discretized with a finite volume technique, while the second equation is of parabolic type and is easily discretized with a symmetric positive diffusion matrix. The implicit linear system can be solved with a conjugate gradient algorithm, which reveals very powerful (both in term of accuracy and speed) for this problem.

3. Splitted approximations of the M^1 model

Our aim is at the description of splitted approximation of the M^1 model, in view of the discretization of (2) such that (7) is by construction an asymptotic limit of the scheme. We also take care of the natural reality condition that says that $\frac{|F_r|}{E_r} \leqslant 1$. This comes from $\frac{|F_r|}{E_r} = \frac{|\int\int nI(v,n)\ \mathrm{d}v\ \mathrm{d}n|}{\int\int I(v,n)\ \mathrm{d}v\ \mathrm{d}n} \leqslant 1$ for a smooth smooth intensity I. Straightforward but lengthy calculations show that

Proposition 1. *Assuming that $T_r > 0$ then*

$$|b| < 1 \Longleftrightarrow \frac{|Q_r|}{S_r} < 1 \Longleftrightarrow \frac{|F_r|}{E_r} < 1. \tag{11}$$

From (3) and (4) it is sufficient to prove that : $-1 < b < 1$ implies $-1 < \frac{4b}{3+b^2} < 1$. The range $-1 < b < 1$ is the physical range in which the physical solution is searched. The inequalities are strict because the map $(E_r, F_r) \to (S_r, Q_r)$ is singular at $b = \pm 1$. A convenient way to extend the range to $-1 \leqslant b \leqslant 1$ is proposed in Section 3.2.

3.1. Splitting method for the M^1 model

We generalize the splitting method of (10). The first part of the splitting is written as

$$\begin{aligned} &\frac{\partial}{\partial t} S_r + \frac{\partial}{\partial x} v S_r = 0, \\ &\frac{\partial}{\partial t} Q_r + \frac{\partial}{\partial x} v Q_r = 0. \end{aligned} \tag{12}$$

The first equation is natural, in the sense that it is the first equation of (10). The second equation is arbitrary: notice however that a consequence will be the compatibility with the realizability condition (11).

Proposition 2. *Assume the velocity filed v is smooth. Assume that $\frac{|Q_r|}{S_r} < 1$ for all x at $t = 0$. Then $\frac{|Q_r|}{S_r} < 1$ for all x and for all $t > 0$.*

A algebraic consequence of (12) is $\frac{\partial Q_r}{\partial t S_r} + v\frac{\partial Q_r}{\partial x S_r} = 0$. So the parameter $b = -\frac{Q_r}{S_r}$ is just transported by the equation. It ends the proof.

Proposition 3. *The system (12) is algebraically equivalent to*

$$\begin{aligned} &\frac{\partial}{\partial t}E_r + \frac{\partial}{\partial x}vE_r + \frac{1}{3}E_r\frac{\partial}{\partial x}v = 0,\\ &\frac{\partial}{\partial t}F_r + \frac{\partial}{\partial x}vF_r + \frac{1}{3}F_r\frac{\partial}{\partial x}v = 0. \end{aligned} \tag{13}$$

A proof is as follows. The system (12) is also $\frac{\partial}{\partial t}S_r + v\frac{\partial}{\partial x}S_r + S_r\frac{\partial}{\partial x}v = 0$ and $\frac{\partial}{\partial t}Q_r + v\frac{\partial}{\partial x}Q_r + Q_r\frac{\partial}{\partial x}v = 0$. Since one has $\mathrm{d}E_r = \frac{\partial E_r}{\partial S_r}\mathrm{d}S_r + \frac{\partial E_r}{\partial Q_r}\mathrm{d}Q_r$ then

$$\frac{\partial}{\partial t}E_r + v\frac{\partial}{\partial x}E_r + \left(\frac{\partial E_r}{\partial S_r}S_r + \frac{\partial E_r}{\partial Q_r}Q_r\right)\frac{\partial}{\partial x}v = 0. \tag{14}$$

From its definition one has $E_r = S_r^{\frac{4}{3}}\varphi(\frac{Q_r}{S_r})$. Then

$$\frac{\partial E_r}{\partial S_r}S_r + \frac{\partial E_r}{\partial Q_r}Q_r = \left(\frac{4}{3}S_r^{\frac{1}{3}} \times \varphi\left(\frac{Q_r}{S_r}\right) - S_r^{\frac{4}{3}}\frac{Q_r}{S_r^2}\varphi'\left(\frac{Q_r}{S_r}\right)\right)S_r + \left(S_r^{\frac{4}{3}}\frac{1}{S_r}\varphi'\left(\frac{Q_r}{S_r}\right)\right)Q_r = \frac{4}{3}E_r.$$

Using this in (14) it gives the first equation of (13). Concerning the second equation in (13) we note that $F_r = S_r^{\frac{4}{3}}\psi(\frac{Q_r}{S_r})$. Therefore, a similar algebra ends the proof of the proposition.

Now we subtract (13) to the M^1 model (2). This subtraction allows to reconstruct (2) using the splitting method. The subtraction is valid only for the derivatives in space, and not in time. We get

$$\begin{aligned} &\frac{\partial}{\partial t}E_r + \frac{\partial}{\partial x}\left(\frac{F_r}{\varepsilon} - vE_r\right) - \frac{E_r}{3}\frac{\partial}{\partial x}v = S_E,\\ &\frac{\partial}{\partial t}F_r + \frac{\partial}{\partial x}\left(\frac{P_r}{\varepsilon} - vF_r\right) - \frac{F_r}{3}\frac{\partial}{\partial x}v = S_F. \end{aligned} \tag{15}$$

We claim that the non-equilibrium diffusion limit of (15) is (6) but with $v \equiv 0$. This property means that the splitting method has really subtract the drift effect due to the Lorentzian compatibility of the model.

Proposition 4. *Whatever v is, the non-equilibrium diffusion limit ($\sigma_a = O(\varepsilon^2)$ and $\sigma_s = O(1)$) of the system (15) is the second equation of (10), that is*

$$\frac{\partial}{\partial t}E_r + \frac{\partial}{\partial x}\left(-\frac{1}{\sigma_s}\frac{\partial}{\partial x}E_r\right) = \sigma_a(T^4 - E_r). \tag{16}$$

This property means that if we set $v = 0$ in (15) then we respect the non-equilibrium diffusion limit of the M^1 model, provided we use the splitting method. If $v \equiv 0$ the system (15) is the standard radiation M^1 model with the matter at rest.

The splitted model is made of (12) followed by (15) where we have set $v = 0$. This model is composed of (12) followed by

$$\begin{aligned} &\frac{\partial}{\partial t}E_r + \frac{\partial}{\partial x}\left(\frac{F_r}{\varepsilon}\right) = \frac{\sigma_a}{\varepsilon^2}(T^4 - E_r),\\ &\frac{\partial}{\partial t}F_r + \frac{\partial}{\partial x}\left(\frac{P_r}{\varepsilon}\right) = -\frac{\sigma_a + \sigma_s}{\varepsilon^2}F_r. \end{aligned} \tag{17}$$

In the numerical section we will show how to derive accurate and robust schemes for the discretization of (12)–(17).

3.2. Elimination of the singularity near $|f| = 1$

The method of moment is singular near $f = \pm 1$ since in this case T_r is zero for finite E_r, see formula (3). It simply means that, far from isotropy, T_r is not a temperature and is only a parameter of the generalized Planckian. At the numerical level we prefer to use non-singular equations near $f = \pm 1$. We think this is important to get accurate numerical results if f is close to 1, because singular equations are most of time difficult to discretize correctly.

We notice that it is sufficient to redefine $S_r = E_r^{\frac{3}{4}}$ and $Q_r = -bE_r^{\frac{3}{4}}$, because (12) is equivalent to $(\partial_t + v\partial_x)b = 0$ and $\partial_t T_r^3 + \partial_x(vT_R^3) = 0$. This transformation is a smooth map between (E_r, F_r) and $(S_r, Q_r) = (E_r^{\frac{3}{4}}, -bE_r^{\frac{3}{4}})$. From now on the splitted approximation we use is

$$\begin{aligned} &\frac{\partial}{\partial t} S_r + \frac{\partial}{\partial x} v S_r = 0, \quad S_r = E_r^{\frac{3}{4}}, \\ &\frac{\partial}{\partial t} Q_r + \frac{\partial}{\partial x} v Q_r = 0, \quad Q_r = -bE_r^{\frac{3}{4}}. \end{aligned} \tag{18}$$

followed by

$$\begin{aligned} &\frac{\partial}{\partial t} E_r + \frac{\partial}{\partial x}\left(\frac{F_r}{\varepsilon}\right) = \frac{\sigma_a}{\varepsilon^2}(T^4 - E_r), \\ &\frac{\partial}{\partial t} F_r + \frac{\partial}{\partial x}\left(\frac{P_r}{\varepsilon}\right) = -\frac{\sigma_a + \sigma_s}{\varepsilon^2} F_r. \end{aligned} \tag{19}$$

3.3. Extension for radiation hydrodynamics

Written in non-dimensional variables the model we use is

$$\begin{aligned} &\frac{\partial}{\partial t}(\rho) + \frac{\partial}{\partial x}(\rho v) = 0, \\ &\frac{\partial}{\partial t}(\rho v) + \frac{\partial}{\partial x}\left(\rho v^2 + p + \frac{E_r}{3}\right) = 0, \\ &\frac{\partial}{\partial t}(\rho E + E_r) + \frac{\partial}{\partial x}\left(\rho E v + p v + \frac{E_r}{3} v + \frac{1}{\varepsilon} F_r\right) = 0, \\ &\frac{1}{\varepsilon}\frac{\partial}{\partial t} E_r + \partial_x(v E_r) + \frac{E_r}{3}\partial_x v + \frac{\partial}{\partial x} F_r = \frac{\sigma_a}{\varepsilon^2}(T^4 - E_r), \\ &\frac{1}{\varepsilon}\frac{\partial}{\partial t} F_r + \partial_x(v F_r) + \frac{F_r}{3}\partial_x v + \frac{\partial}{\partial x} P_r = -\frac{\sigma_a + \sigma_s}{\varepsilon^2} F_r, \end{aligned} \tag{20}$$

where the source terms are $O(\frac{1}{\varepsilon^2})$ in opaque materials and are negligible in transparent materials. In view of the previous analysis, we propose to split the radiative solver from the hydrodynamics solver. It means that (20) is solved using

$$\begin{aligned} &\frac{\partial}{\partial t}(\rho) + \frac{\partial}{\partial x}(\rho v) = 0, \\ &\frac{\partial}{\partial t}(\rho v) + \frac{\partial}{\partial x}\left(\rho v^2 + p + \frac{E_r}{3}\right) = 0, \\ &\frac{\partial}{\partial t}(\rho E + E_r) + \frac{\partial}{\partial x}\left(\rho E v + p v + \frac{E_r}{3} v\right) = 0, \\ &\frac{\partial}{\partial t} S_r + \frac{\partial}{\partial x}(u S_r) = 0, \quad S_r = E_r^{\frac{3}{4}}, \\ &\frac{\partial}{\partial t} Q_r + \frac{\partial}{\partial x}(u Q_r) = 0, \quad Q_r = -bS_r, \end{aligned} \tag{21}$$

with b defined by (3), and followed by

$$\begin{aligned}
&\partial_t E_r + \frac{1}{\varepsilon}\partial_x F_r = \sigma_a \frac{T^4 - E_r}{\varepsilon^2},\\
&\partial_t F_r + \frac{1}{\varepsilon}\partial_x P_r = -\sigma_t \frac{F_r}{\varepsilon^2}, \quad \sigma_t = \sigma_a + \sigma_s,\\
&\rho C_v \partial_t T = \sigma_a \frac{E_r - T^4}{\varepsilon^2}.
\end{aligned} \tag{22}$$

It is possible to treat directly the radiative moment system. We think our approach is simpler to capture the diffusion limit of the model.

4. Derivation of the numerical schemes

The time step is $\Delta t > 0$, the mesh size is $\Delta x > 0$, the value of the radiative energy and flux in the cell $](j-\frac{1}{2})\Delta x, (j+\frac{1}{2})\Delta x[$ and at time step n is denoted as $(E_r^{j,n}, F_r^{j,n})$. Similarly, the radiative entropy and radiative entropy flux are $(S_r^{j,n}, Q_r^{j,n})$. The velocity $u^n_{j+\frac{1}{2}}$ is assumed to be known at each interface and at each time step.

4.1. Discretization of (18)

The discretization is quite natural in the context of finite volume method. Many methods exist. For the sake of completeness we describe the most simple one. We assume that $u^n_{j+\frac{1}{2}} \geqslant 0$ for all (j, n), so that the up-winding is uniform. With this hypothesis, the scheme is

$$\begin{aligned}
&\frac{S_r^{j,n+1} - S_r^{j,n}}{\Delta t} + \frac{u^n_{j+\frac{1}{2}} S_r^{j,n} - u^n_{j-\frac{1}{2}} S_r^{j-1,n}}{\Delta x} = 0,\\
&\frac{Q_r^{j,n+1} - Q_r^{j,n}}{\Delta t} + \frac{u^n_{j+\frac{1}{2}} Q_r^{j,n} - u^n_{j-\frac{1}{2}} Q_r^{j-1,n}}{\Delta x} = 0.
\end{aligned} \tag{23}$$

Proposition 5. *Assume that* $\frac{|Q_r^{j,n}|}{S_r^{j,n}} \leqslant 1$ *for all j. Assume the CFL condition* $(\max_j u^n_{j+\frac{1}{2}})\Delta t \leqslant \Delta x$. *Then one has* $\frac{|Q_r^{j,n+1}|}{S_r^{j,n+1}} \leqslant 1$ *for all j.*

Let us use simplified notations for the sake of convenience : $\alpha = S_r - Q_r$ and $\beta = S_r + Q_r$. Then α and β satisfy the same discrete equations, which implies the positivily under CFL.

4.2. Discretization of the radiative step (22)

In this part we explain the main features of the scheme we propose for the discretization of the (22). First, we show that a direct linear implicitation of the HLL like solvers leads to a non-positive linear implicit problem. Second, we modify the HLL solver and introduce a new scheme. We show that the modification fixes the positivity of the scheme. For expository purposes we take $\sigma_a = \sigma_s = 0$ when dealing with the HLL solver and $\sigma_a = 0$, $\sigma_s \geqslant 0$ for the new scheme. Finally, we consider the general case $\sigma_a \geqslant 0$ and $\sigma_s \geqslant 0$. The general method is to use the theory of M-matrices.

Since we describe and analyze implicit schemes, the boundary conditions are important because they modify the coefficients of the linear system. A bad discretization may pollute the M-matrix structure.

4.2.1. A basic example of a non-positive implicit solver

We begin with a simple basic example which shows that a direct implicitation is a priori non-positive. Let us freeze the Eddington factor in (22) and take $\sigma \equiv 0$

$$\begin{aligned}
&\frac{\partial}{\partial t}E_{\rm r}+\frac{\partial}{\partial x}\left(\frac{F_{\rm r}}{\varepsilon}\right)=0,\\
&\frac{\partial}{\partial t}F_{\rm r}+\frac{\partial}{\partial x}\left(\frac{a^2E_{\rm r}}{\varepsilon}\right)=0.
\end{aligned}\tag{24}$$

Here the coefficient a is the square root of the Eddington factor defined by $a^2=\frac{P_{\rm r}}{E_{\rm r}}\in[\frac{1}{3},1]$. Then we discretize (24) with a standard approximate Godunov method, the so-called HHL scheme which is described in [34, p. 298]. Since the maximum wave speed is $\frac{1}{\varepsilon}$ the scheme is

$$\begin{aligned}
&\frac{E_{\rm r}^{j,n+1}-E_{\rm r}^{j,n}}{\Delta t}+\frac{1}{\varepsilon}\frac{F_{\rm r}^{j+\frac12,n+1}-F_{\rm r}^{j-\frac12,n+1}}{\Delta x}=0,\\
&\frac{F_{\rm r}^{j,n+1}-F_{\rm r}^{j,n}}{\Delta t}+\frac{1}{\varepsilon}\frac{(a^2E)^{j+\frac12,n+1}-(a^2E)^{j-\frac12,n+1}}{\Delta x}=0.
\end{aligned}\tag{25}$$

The inter-facial flux is given by the first order finite volume approximation

$$\begin{aligned}
&(a^2E)^{j+\frac12,n+1}=\frac{(a_j^2E_r^{j,n+1}+a_{j+1}^2E_r^{j+1,n+1})+F_{\rm r}^{j,n+1}-F_{\rm r}^{j+1,n+1}}{2},\\
&F_{\rm r}^{j+\frac12,n+1}=\frac{F_{\rm r}^{j,n+1}+F_{\rm r}^{j+1,n+1}+E_{\rm r}^{j,n+1}-E_{\rm r}^{j+1,n+1}}{2}.
\end{aligned}\tag{26}$$

This is an implicit linear system that we solve with a direct solver in dimension one. A conjugate gradient solver can be used if needed in dimension two and more. Unfortunately, this scheme does not necessarily respect the flux limiting property. The scheme may be *non-positive*. To show this, we rely on the theory of M matrices [3]. This theory provide necessary and sufficient conditions such that the solution of a general linear system $\mathscr{A}x=b$ gives a non-negative solution $x\geqslant 0$ for all $b\geqslant 0$. Here $x\geqslant 0$ means that $x_i\geqslant 0$ for all i. We retain the simple condition on $\mathscr{A}$

$$\text{if } a_{ij}\leqslant 0\quad \forall i\neq j,\quad \text{and}\quad \left(\sum_j a_{ij}>0\ \forall i \text{ or } \sum_i a_{ij}>0\ \forall j\right)$$

then $\mathscr{A}$ is an M-matrix with $x=\mathscr{A}^{-1}b\geqslant 0$ for all $b\geqslant 0$. The flux limited condition $|F_{\rm r}|\leqslant E_{\rm r}$ is equivalent to the positivity of $u=E_{\rm r}+F_{\rm r}$ and $v=E_{\rm r}-F_{\rm r}$. Therefore, we check the property of M matrix for the system (25) with the flux defined by (26) and for the unknown $x=(u^{j,n+1},v^{j,\ n+1})_j$ and the right-hand side $b=(u^{j,n},v^{j,n})_j$. For the sake of simplicity assume that $\sigma\equiv 0$ so that $M\equiv 1$. The equation for $v^{j,n+1}$ is

$$\begin{aligned}
&\frac{v^{j,n+1}-v^{j,n}}{\Delta t}+\frac{1}{4\varepsilon\Delta x}\left(\left(1-a_{j+\frac12}^2\right)u^{j+1,n+1}+\left(a_{j-\frac12}^2-1\right)u^{j-1,n+1}+\left(-3-a_{j+\frac12}^2\right)v^{j+1,n+1}\right.\\
&\left.+\left(-1-a_{j-\frac12}^2\right)v^{j-1,n+1}+4v^{j,n+1}\right)=0.
\end{aligned}$$

If $a_{j+\frac12}<1$ the extra-diagonal coefficient in front of $u^{j+1,n+1}$ has the wrong sign. There is a similar property for the equation that gives $u^{j,n+1}$. Therefore, the solution of the linear system can be non-positive.

It is worthwhile to notice that the explicit scheme is positive. The equation becomes

$$\begin{aligned}
&\frac{v^{j,n+1}-v^{j,n}}{\Delta t}+\frac{1}{4\varepsilon\Delta x}\left(\left(1-a_{j+\frac12}^2\right)v^{j+1,n}+\left(a_{j-\frac12}^2-1\right)v^{j-1,n}+\left(-3-a_{j+\frac12}^2\right)v^{j+1,n}+\left(-1-a_{j-\frac12}^2\right)v^{j-1,n}+4v^{j,n}\right)\\
&=0.
\end{aligned}$$

One can check that $(1-a_{j+\frac12}^2)u^{j+1,n}+(a_{j-\frac12}^2-1)u^{j-1,n}\leqslant 0$ because $a_j^2=a(\frac{F_{\rm r}^{j,n}}{E_{\rm R}^{j,n}})^2\geqslant 2|\frac{F_{\rm r}^{j,n}}{E_{\rm R}^{j,n}}|-1$. Nevertheless the explicit scheme is restricted by the explicit CFL condition $\frac{\Delta t}{\varepsilon\Delta x}\leqslant 1$. This is why we propose in the following a new linear implicit AP and unconditionally positive scheme.

4.2.2. AP and positive discretization of (22) with $\sigma_a=0$

The idea is to use use a strategy that has been proposed and used in [6,7]. It consists in a linearization of the system combined with a well balanced scheme. Depending on the linearization, it is possible to design different

numerical schemes with slightly different theoretical properties. In order to simplify the presentation, we consider (24). We will indicate later on how to deal with the temperature relaxation. Here we use a strategy that has been first proposed and used in [6,7]. It consists in the use of a relaxation method (see for example [16] for principle of relaxation method) to "linearize" the system and a "well-balanced" scheme. This combination gives stability and preservation of the asymptotic limit.

Let us first define the relaxation method. We introduce the intermediate relaxation unknowns $X = \frac{F_r}{a}$ and $Y = \frac{P_r}{a}$ and we consider the system

$$\begin{aligned} &\frac{\partial}{\partial t}E_r + \frac{1}{\varepsilon}\frac{\partial}{\partial x}aX = 0,\\ &\frac{\partial}{\partial t}X + \frac{1}{\varepsilon}\frac{\partial}{\partial x}aE_r = -\frac{\sigma}{\varepsilon^2}X + \frac{1}{\lambda}\left(\frac{F_r}{a} - X\right), \end{aligned} \tag{27}$$

and

$$\begin{aligned} &\frac{\partial}{\partial t}Y + \frac{1}{\varepsilon}\frac{\partial}{\partial x}aF_r = 0,\\ &\frac{\partial}{\partial t}F_r + \frac{1}{\varepsilon}\frac{\partial}{\partial x}aY = -\frac{\sigma}{\varepsilon^2}F_r + \frac{1}{\lambda}\left(\frac{P_r}{a} - Y\right). \end{aligned} \tag{28}$$

The coefficient a is the square root of the Eddington factor defined by $a^2 = \frac{P_r}{E_r}$. The additional variables are $X \approx \frac{F_r}{a}$ and $Y \approx \frac{P_r}{a}$. More exactly if the relaxation coefficient λ tends to 0, then $X \to \frac{F_r}{a}$ and $Y \to \frac{P_r}{a}$, and the asymptotic limit is indeed (19). In the original work [6,7], the relaxation variables were $X = F_r$ and $Y = P_r$. Our choice has better properties.

As it is usually done, we consider the relaxed version of (27). This is no more that using a splitting technique to solve (27), by splitting the relaxation source from the rest and let formally λ tends to 0 in the relaxation step. This leads to the following transport-projection algorithm:

- *Transport step*: let $a = \sqrt{\chi^n}$ $X^n = \frac{F_r^n}{a}$ and $Y^n = \frac{P_r^n}{a}$ at the beginning of the time step. Then we solve the systems

$$\begin{aligned} &\frac{\partial}{\partial t}E_r + \frac{1}{\varepsilon}\frac{\partial}{\partial x}aX = 0,\\ &\frac{\partial}{\partial t}X + \frac{1}{\varepsilon}\frac{\partial}{\partial x}aE_r = -\frac{\sigma}{\varepsilon^2}X, \end{aligned} \tag{29}$$

  and

$$\begin{aligned} &\frac{\partial}{\partial t}Y + \frac{1}{\varepsilon}\frac{\partial}{\partial x}aF_r = 0,\\ &\frac{\partial}{\partial t}F_r + \frac{1}{\varepsilon}\frac{\partial}{\partial x}aY = -\frac{\sigma}{\varepsilon^2}F_r, \end{aligned} \tag{30}$$

  during one time step. So we know the initial conditions at $n\Delta t$ and we use (29) and (30) to compute all quantities at $(n+1)\Delta t$: that is E_r^{n+1}, F_r^{n+1}, X^{n+1} and Y^{n+1}.
- *Projection step*: we drop X^{n+1} and Y^{n+1} and reinitialize $a = \sqrt{\chi^{n+1}}$, $X^{n+1} = \frac{F_r^{n+1}}{a}$ and $Y^{n+1} = \frac{P_r^{n+1}}{a}$.

Therefore, it remains to explain how we discretize (29) and (30) and what advantages come from this strategy. One can remark that (29) and (30) are decoupled.The method we use for (29) or (30) comes from the work [11–13] about well-balanced schemes for hyperbolic systems with source terms. Originally the goal of this technique was to preserve stationary solutions. Essentially it consists in collapsing the source terms at interfaces and to write down the Godunov method. This step needs the computation of the solution of a Riemann problem with a Dirac source term at the interface. This is quite easy to for linear equations. We refer to [12] for the construction of the method, and to [7] for a simple explanation in the linear case. In what follows we only describe the result of the application of the method to our case.

We have decided to present the scheme with natural notations, such that the consistency of the scheme becomes clear. The coefficient $M_{j+\frac{1}{2}}$is defined on the interfaces by

$$M_{j+\frac{1}{2}} = \frac{2a_{j+\frac{1}{2}}\varepsilon}{\sigma_{j+\frac{1}{2}}\Delta x + 2a_{j+\frac{1}{2}}\varepsilon} \tag{31}$$

where quantities of the type $q_{j+\frac{1}{2}}$ are mean value of q_j and q_{j+1}. Then we discretize (29) with

$$\begin{aligned}
&\frac{E_{\mathrm{r}}^{j,n+1} - E_{\mathrm{r}}^{j,n}}{\Delta t} + \frac{1}{\varepsilon}\frac{M_{j+\frac{1}{2}}a_{j+\frac{1}{2}}X^{j+\frac{1}{2},n+1} - M_{j-\frac{1}{2}}a_{j-\frac{1}{2}}X^{j-\frac{1}{2},n+1}}{\Delta x} = 0,\\
&\frac{X^{j,n+1} - X^{j,n}}{\Delta t} + \frac{1}{\varepsilon}\frac{M_{j+\frac{1}{2}}a_{j+\frac{1}{2}}E^{j+\frac{1}{2},n+1} - M_{j-\frac{1}{2}}a_{j-\frac{1}{2}}E^{j-\frac{1}{2},n+1}}{\Delta x}\\
&\quad = -\frac{1}{2}\left(M_{j+\frac{1}{2}}\frac{a_j}{a_{j+\frac{1}{2}}}\frac{\sigma_{j+\frac{1}{2}}}{\varepsilon^2} + M_{j-\frac{1}{2}}\frac{a_j}{a_{j-\frac{1}{2}}}\frac{\sigma_{j-\frac{1}{2}}}{\varepsilon^2}\right)X_i^{n+1} + \frac{M_{j+\frac{1}{2}} - M_{j-\frac{1}{2}}}{\varepsilon\Delta x}a_iE_i^{n+1}.
\end{aligned} \tag{32}$$

The initial value of the additional unknown X is $X^{j,n} = \frac{F_{\mathrm{r}}^{j,n}}{a_j}$. The fluxes are

$$\begin{aligned}
a_{j+\frac{1}{2}}E^{j+\frac{1}{2},n+1} &= \frac{a_jE^{j,n+1} + a_{j+1}E^{j+1,n+1}}{2} + \frac{a_jX^{j,n+1} - a_{j+1}X^{j+1,n+1}}{2},\\
a_{j+\frac{1}{2}}X^{j+\frac{1}{2},n+1} &= \frac{a_jX^{j,n+1} + a_{j+1}X^{j+1,n+1}}{2} + \frac{a_jE^{j,n+1} - a_{j+1}E^{j+1,n+1}}{2}.
\end{aligned} \tag{33}$$

The linear scheme (32) and (33) is implicit and can easily be solved in 1D. For the system (30), the scheme is exactly the same except that E_{r} is replaced by Y and that X is replaced by F_{r}. Nevertheless the initialization of the Y variable is $Y^{j,n} = \frac{P_{\mathrm{r}}^{j,n}}{a_j}$.

Proposition 6 (The scheme is AP). *Assume that $\sigma = \mathrm{O}(1)$ and ε is small. Then the diffusion limit of the scheme (25) is*

$$\frac{E_{\mathrm{r}}^{j,n+1} - E_{\mathrm{r}}^{j,n}}{\Delta t} - \frac{\frac{1}{3\sigma_{j+\frac{1}{2}}}(E_{\mathrm{r}}^{j+1,n+1} - E_{\mathrm{r}}^{j,n+1}) - \frac{1}{3\sigma_{j-\frac{1}{2}}}(E_{\mathrm{r}}^{j,n+1} - E_{\mathrm{r}}^{j-1,n+1})}{\Delta x^2} = 0. \tag{34}$$

The second equation in (25) implies that $F_{\mathrm{r}}^{j,n+1}$ is small of order $\varepsilon : F_{\mathrm{r}}^{j,n+1} = \mathrm{O}(\varepsilon)$. Since this is true for all j and n, then the Eddington factor is close to one third $a^2 = \frac{1}{3} + \mathrm{O}(\varepsilon)$ for all j and n. Then

$$M_{j+\frac{1}{2}} = \frac{2\frac{1}{\sqrt{3}}\varepsilon}{\sigma_{j+\frac{1}{2}}\Delta x} + \mathrm{O}(\varepsilon^{\frac{3}{2}}). \tag{35}$$

So the flux that matters in (25) is up to $\mathrm{O}(\varepsilon)$

$$\frac{M_{j+\frac{1}{2}}}{\varepsilon}F_{\mathrm{r}}^{j+\frac{1}{2},n+1} = \frac{\frac{1}{\sqrt{3}}\frac{2\frac{1}{\sqrt{3}}\varepsilon}{\sigma_{j+\frac{1}{2}}\Delta x}(E_{\mathrm{r}}^{j+1,n+1} - E_{\mathrm{r}}^{j,n+1})}{2} = \frac{E_{\mathrm{r}}^{j+1,n+1} - E_{\mathrm{r}}^{j,n+1}}{3\sigma_{j+\frac{1}{2}}\Delta x}.$$

It ends the proof.

It is particularly convenient to use the diagonal form of the system. Let $u = E_{\mathrm{r}} + X$ and $v = E_{\mathrm{r}} - X$. The equations can be written as a system in $x = (u, v)$

$$\begin{aligned}
&\frac{u^{j,n+1} - u^{j,n}}{\Delta t} + \frac{M_{j-\frac{1}{2}}}{\varepsilon}\frac{a_ju^{j,n+1} - a_{j-1}u^{j-1,n+1}}{\Delta x} = M_{j-\frac{1}{2}}\frac{a_j}{a_{j-\frac{1}{2}}}\frac{\sigma_{j-\frac{1}{2}}}{2\varepsilon^2}(v^{j,n+1} - u^{j,n+1}),\\
&\frac{v^{j,n+1} - v^{j,n}}{\Delta t} - \frac{M_{j+\frac{1}{2}}}{\varepsilon}\frac{a_{j+1}v^{j+1,n+1} - a_jv^{j,n+1}}{\Delta x} = M_{j+\frac{1}{2}}\frac{a_j}{a_{j+\frac{1}{2}}}\frac{\sigma_{j+\frac{1}{2}}}{2\varepsilon^2}(u^{j,n+1} - v^{j,n+1}).
\end{aligned} \tag{36}$$

In view of (36) the natural discrete boundary conditions are

$$\begin{aligned}
&j = 1 : \ a_{j-1}u^{j-i,n+1} = \alpha_1a_jv^{j,n+1} + \alpha_2 \quad \text{with } \alpha_1, \alpha_2 \geqslant 0,\\
&j = N : \ a_{j+1}v^{j+i,n+1} = \alpha_3a_ju^{j,n+1} + \alpha_4 \quad \text{with } \alpha_3, \alpha_4 \geqslant 0.
\end{aligned} \tag{37}$$

Plugging the boundary conditions (37) inside the scheme (36) the linear system can be written as

$$\mathscr{A}x = b, \quad \mathscr{A} = I - \Delta t M^{\mathrm{S}} - \Delta t M^{\mathrm{BC}}, \tag{38}$$

where M^{S} is the matrix of the scheme, and M^{BC} is for the boundary conditions. The matrix $\mathscr{A}$ is not symmetric. The right-hand side is $b = x^n + \Delta t(\alpha_2, 0, \ldots, 0, \alpha_4)$. By construction one has the property $M^{\mathrm{S}}_{ii} \leqslant 0$, $M^{\mathrm{S}}_{ij} \geqslant 0$ for $i \neq j$ and $\sum_i M^{\mathrm{S}}_{ij} \leqslant 0$ and (this is trivial) $M^{\mathrm{BC}}_{ii} \leqslant 0$, $M^{\mathrm{BC}}_{ij} \geqslant 0$ for $i \neq j$ and $\sum_i M^{\mathrm{BC}}_{ij} \leqslant 0$. The inequality $\sum_i M^{\mathrm{S}}_{ij} \leqslant 0$ is an equality inside the domain: $\sum_i M^{\mathrm{S}}_{ij} = 0$ for $2 \leqslant j \leqslant N-1$. Therefore, the diagonal of $\mathscr{A}$ is strictly dominant with respect to the columns inside the domain. It is of particular interest to show that diagonal of $\mathscr{A}$ is also dominant at the boundaries. It is the case for incoming boundary conditions for which $\alpha_1 = \alpha_3 = 0$. For transparent conditions one has also $\alpha_2 = \alpha_4 = 0$. For general boundary conditions the property is guaranteed if $0 \leqslant \alpha_1 \leqslant 1$ and $0 \leqslant \alpha_3 \leqslant 1$: we note this property comes from the dissipative nature of the boundary conditions. From now on, we assume that

$$\mathscr{A}_{ij} \leqslant 0 \quad \text{for } i \neq j, \text{ and } \sum_i \mathscr{A}_{ij} > 0 \quad \forall j.$$

Therefore, the matrix $\mathscr{A}$ is an M-matrix. A general reference is [3]. That is $\mathscr{A}$ is invertible and $\mathscr{A}^{-1} \geqslant 0$.

Proposition 7 (The scheme is positive). *Assume that $E^{j,n}_{\mathrm{r}} \pm F^{j,n}_{\mathrm{r}} \geqslant 0$ for all j. Then $E^{j,n+1}_{\mathrm{r}} \pm F^{j,n+1}_{\mathrm{r}} \geqslant 0$ for all j.*

This flux limited property is the reason why we prefer to use this relaxation method rather than the direct approach (26). The price to pay is that we need to solve two linear systems with twice the number of unknowns when compared with (26). The linear systems are absolutely identical. We divide the proof of Proposition 7 in three steps.

(a) *Claim that $E^{j,n+1}_{\mathrm{r}} \pm X^{j,n+1} \geqslant 0$.* The proof consists in writing the equation for $u = E_{\mathrm{r}} + X$ and $v = E_{\mathrm{r}} - X$. This set of linear equations can be rewritten as $\mathscr{A}x = b$ where $\mathscr{A}$ is the matrix of the system, $x = (u^{j,n+1}, v^{j,n+1})$ is the unknown of the linear system and $b = (u^{j,n}, v^{j,n})$ is the right-hand side of the linear system. To prove the claim it is sufficient to prove that all component of x are non-negative. First, we assume that all component of b are non-negative, which is due to the hypothesis: $\frac{|X^{j,n}|}{E^{j,n}_{\mathrm{r}}} = \frac{|F^{j,n}_{\mathrm{r}}|}{a_j E^{j,n}_{\mathrm{r}}} \leqslant 1$. Second, we us the M-matrix property. It proves the claim $u^{j,n+1} = E^{j,n+1}_{\mathrm{r}} + X^{j,n+1} \geqslant 0$ and $v^{j,n+1} = E^{j,n+1}_{\mathrm{r}} - X^{j,n+1} \geqslant 0$.

(b) *Claim that $Y^{j,n+1}_{\mathrm{r}} \pm F^{j,n+1}_{\mathrm{r}} \geqslant 0$.* We use the same method. Let $w = Y + F_{\mathrm{r}}$ and $z = Y - F_{\mathrm{r}}$. Then $w^{j,n} = Y^{j,n} + F^{j,n}_{\mathrm{r}} = \frac{P^{j,n}_{\mathrm{r}}}{a_j} + F^{j,n}_{\mathrm{r}} = a_j E^{j,n}(a_j + \frac{F^{j,n}_{\mathrm{r}}}{E^{j,n}})$. Since a_j is a function of the non-dimensional radiation flux $\frac{F^{j,n}_{\mathrm{r}}}{E^{j,n}}$, then it is sufficient to study the function $f \mapsto a = \sqrt{\chi}$. Since $\chi - f^2 = \frac{(1-\sqrt{4-3f^2})^2}{3} \geqslant 0$, then $a \geqslant |f|$ and therefore $w^{j,n} \geqslant 0$. Similarly, $z^{j,n} \geqslant 0$. The new values $x' = (w^{j,n+1}, z^{j,n+1})$ are solutions of the same linear linear system, $\mathscr{A}x' = b'$ where $b' = (w^{j,n}, z^{j,n})$. Since $b' \geqslant 0$ then x' also. Therefore, $w^{j,n+1}, z^{j,n+1} \geqslant 0$.

(c) *Claim that $E^{j,n+1}_{\mathrm{r}} \pm F^{j,n+1}_{\mathrm{r}} \geqslant 0$.* Let us define $r = E - Y + X - F$ and $s = E - Y - (X - F)$. Since E, X and Y, F are by definition solutions of the same linear system (32) but with a different initialization of course, then the same method can be used to study the non-negativity of $r^{j,n+1}, s^{j,n+1}$. It is sufficient to check that $r^{j,n}, s^{j,n}$ are non-negative at the beginning of the time step. One has

$$r^n = E^n_{\mathrm{r}} - aE^n_{\mathrm{r}} + \frac{F^n_{\mathrm{r}}}{a} - F^n_{\mathrm{r}} = (1-a)(E^n_{\mathrm{r}} + \frac{F^n_{\mathrm{r}}}{a}) \geqslant 0,$$
$$s^n = E^n_{\mathrm{r}} - aE^n_{\mathrm{r}} - \frac{F^n_{\mathrm{r}}}{a} + F^n_{\mathrm{r}} = (1-a)(E^n_{\mathrm{r}} + \frac{F^n_{\mathrm{r}}}{a}) \geqslant 0.$$

Therefore, $r^{n+1} \geqslant 0$ and $s^{n+1} \geqslant 0$. At the end of the time step

$$2(E^{n+1}_{\mathrm{r}} - F^{n+1}_{\mathrm{r}}) = r^{n+1} + z^{n+1} + v^{n+1} \geqslant 0,$$
$$2(E^{n+1}_{\mathrm{r}} + F^{n+1}_{\mathrm{r}}) = s^{n+1} + w^{n+1} + u^{n+1} \geqslant 0.$$

4.3. Discretization of the full system (22)

Now we describe the scheme for the full system (22). The main tool is, indeed, the discretization described in Section (4.2.2). Let us define the quantities u, v, w, z as $u = E_r + X$, $v = E_r - X$, $w = Y + F_r$ and $z = Y - F_r$. and let also $\alpha_{j-\frac{1}{2}}(\sigma) = 2M_{j-\frac{1}{2}}(\sigma)\frac{a_j}{a_{j-\frac{1}{2}}}\frac{\sigma_{j-\frac{1}{2}}}{2\varepsilon^2}$ where $M_{j-\frac{1}{2}}(\sigma)$ is defined in (31).

The transport part of the AP-relaxation scheme described in (4.2.2) can be written now, in its diagonalized form, as

$$
\begin{aligned}
&\rho_j C_v \frac{T^{j,n+1}-T^{j,n}}{\Delta t} = \frac{\alpha_{j-\frac{1}{2}}(\sigma_a)+\alpha_{j+\frac{1}{2}}(\sigma_a)}{2}\left(\frac{u^{j,n+1}+v^{j,n+1}}{2} - (T^{j,n+1})^4\right),\\
&\frac{u^{j,n+1}-u^{j,n}}{\Delta t} + \frac{M_{j-\frac{1}{2}}(\sigma_t)}{\varepsilon}\frac{a_j u^{j,n+1} - a_{j-1}u^{j-1,n+1}}{\Delta x}\\
&\quad = \alpha_{j-\frac{1}{2}}(\sigma_a)((T^{j,n+1})^4 - u^{j,n+1}) + \left(\alpha_{j-\frac{1}{2}}(\sigma_t) - \alpha_{j-\frac{1}{2}}(\sigma_a)\right)\frac{v^{j,n+1}-u^{j,n+1}}{2},\\
&\frac{v^{j,n+1}-v^{j,n}}{\Delta t} - \frac{M_{j+\frac{1}{2}}(\sigma_t)}{\varepsilon}\frac{a_{j+1}v^{j+1,n+1} - a_j v^{j,n+1}}{\Delta x}\\
&\quad = \alpha_{j+\frac{1}{2}}(\sigma_a)((T^{j,n+1})^4 - v^{j,n+1}) + \left(\alpha_{j+\frac{1}{2}}(\sigma_t) - \alpha_{j+\frac{1}{2}}(\sigma_a)\right)\frac{u^{j,n+1}-v^{j,n+1}}{2}.
\end{aligned}
\tag{39}
$$

$$
\begin{aligned}
&\frac{w^{j,n+1}-w^{j,n}}{\Delta t} + \frac{M_{j-\frac{1}{2}}(\sigma_t)}{\varepsilon}\frac{a_j w^{j,n+1} - a_{j-1}w^{j-1,n+1}}{\Delta x}\\
&\quad = \alpha_{j-\frac{1}{2}}(\sigma_a)(a_j(T^{j,n+1})^4 - w^{j,n+1}) + \left(\alpha_{j-\frac{1}{2}}(\sigma_t) - \alpha_{j-\frac{1}{2}}(\sigma_a)\right)\frac{z^{j,n+1}-w^{j,n+1}}{2},\\
&\frac{z^{j,n+1}-z^{j,n}}{\Delta t} - \frac{M_{j+\frac{1}{2}}(\sigma_t)}{\varepsilon}\frac{a_{j+1}z^{j+1,n+1} - a_j z^{j,n+1}}{\Delta x}\\
&\quad = \alpha_{j+\frac{1}{2}}(\sigma_a)(a_j(T^{j,n+1})^4 - z^{j,n+1}) + \left(\alpha_{j+\frac{1}{2}}(\sigma_t) - \alpha_{j+\frac{1}{2}}(\sigma_a)\right)\frac{w^{j,n+1}-z^{j,n+1}}{2}.
\end{aligned}
\tag{40}
$$

This discretization remains AP, the proof is as in Section (4.2.2). For an infinite domain, one can also easily check the conservation of the total energy $\rho_j C_v T_j + E_{r,j}$.

During the time step the systems (39) and (40) are, as before, decoupled. But now (39) is a non-linear system. The iterative procedure we use to solve system (39) is based on a fixed point procedure proposed first in [33] for non-equilibrium diffusion model. The basic idea of this fixed point procedure is to use $\Theta = T^4$ as unknown instead of T. In [33], it has been reported good convergence behavior of this method. For convenience the index n at the beginning of the time step has been dropped. Our iterative procedure for (39) is

$$
\begin{aligned}
&\rho_j C_v \mu_j^q \frac{\Theta^{j,q+1}-\Theta^j}{\Delta t} = \frac{\alpha_{j-\frac{1}{2}}(\sigma_a)+\alpha_{j+\frac{1}{2}}(\sigma_a)}{2},\\
&\left(\frac{u^{j,q+1}+v^{j,q+1}}{2} - \Theta^{j,q+1}\right)\frac{u^{j,q+1}-u^j}{\Delta t} + \frac{M_{j-\frac{1}{2}}(\sigma_t)}{\varepsilon}\frac{a_j u^{j,q+1} - a_{j-1}u^{j-1,q+1}}{\Delta x}\\
&\quad = \alpha_{j-\frac{1}{2}}(\sigma_a)\left(\Theta^{j,q+1} - \frac{u^{j,q+1}+v^{j,q+1}}{2}\right) + \alpha_{j-\frac{1}{2}}(\sigma_t)\frac{v^{j,q+1}-u^{j,q+1}}{2},\\
&\frac{v^{j,q+1}-v^j}{\Delta t} - \frac{M_{j+\frac{1}{2}}(\sigma_t)}{\varepsilon}\frac{a_{j+1}v^{j+1,q+1} - a_j v^{j,q+1}}{\Delta x} = \alpha_{j+\frac{1}{2}}(\sigma_a)\left(\Theta^{j,q+1} - \frac{u^{j,q+1}+v^{j,q+1}}{2}\right) + \alpha_{j+\frac{1}{2}}(\sigma_t)\frac{u^{j,q+1}-v^{j,q+1}}{2}.
\end{aligned}
\tag{41}
$$

The coefficient μ_j^q is defined by $\mu_j^q = \frac{T^{j,q}-T^j}{\Theta^{j,q}-\Theta^j}$. By construction we have to solve at each iteration on q a linear system

$$\widetilde{\mathscr{A}}^q \tilde{x}^q = \tilde{b}^q,$$

where $\tilde{x}^q = (\rho C_v \mu^q \Theta^{q+1}, u^{q+1}, v^{q+1})$ and $\tilde{b}^q = (\rho C_v \mu^q \Theta, u, v)$. The matrix $\widetilde{\mathscr{A}}^q$ is an M-matrix.

Therefore, at each iteration q one has the positivity of the material temperature and the flux limited property. Next we show that the algorithm is strictly contracting. By computing the difference between two successive iterates of (41) one has the relation

$$\widetilde{\mathscr{A}}^q \tilde{y}^q = \tilde{c}^q,$$

where $\tilde{y}^q = (\rho C_v \mu^q(\Theta^{q+1} - \theta^q), u^{q+1} - u^q, v^{q+1} - v^q)$ and $\tilde{c}^q = (\rho C_v(\mu^q - \underbrace{\mu}^{q-1})\Theta^q, 0, 0)$. The structure of $\widetilde{\mathscr{A}}^q$ is similar to the structure of $\mathscr{A}$, that is there exists a matrix M^q such that $\widetilde{\mathscr{A}}^q = I - \Delta t M^q$. The important property of M^q is

$$M^q_{ij} \geqslant 0 \quad \text{for } i \neq j, \quad \sum_i M^q_{ij} \leqslant 0.$$

A consequence[2] is as follows: the matrix $(\widetilde{\mathscr{A}}^q)^{-1} \leqslant 1$ is contracting in l^1.

Therefore,

$$\sum_j \left(\rho C_v \mu^q_j |\Theta^{q+1}_j - \Theta^q_j| + \frac{1}{2}|u^{q+1}_j - u^q_j| + \frac{1}{2}|v^{q+1}_j - v^q_j| \right) \leqslant \sum_j (\rho C_v \mu^{q-1}_j |\Theta^q_j - \Theta^{q-1}_j||\beta^q_j|)$$
$$\leqslant (\max_j |\beta^q_j|) \times \sum_j (\rho C_v \mu^{q-1}_j |\Theta^q_j - \Theta^{q-1}_j|),$$

where $\beta^q_j = \frac{\mu^q_j - \mu^{q-1}_j}{\Theta^q_j - \Theta^{q-1}_j} \times \frac{\Theta^q_j}{\mu^{q-1}_j}$ Using the definition of the quantities μ^q_j, one can easily check that, at convergence, this quantity scales like $\beta^q_j \approx \frac{1}{4} \times \frac{3(T^q_j)^3 + 2(T^q_j)^2 T_{j,n} + T^q_j T^2_{j,n}}{(T^q_j)^3 + (T^q_j)^2 T_{j,n} + T^q_j T^2_{j,n} + T^3_{j,n}}$, so $|\beta| < \frac{3}{4}$. Since this number β is the asymptotic value of contraction ratio of the fixed point procedure, it explains why this algorithm is strictly contracting in any neighborhood of the solution. Moreover, all steps of the fixed point procedure are positive (this property was already stressed in the work [33]). In our context it is also a consequence of the M matrix property.

5. Numerical results

All test cases have been performed with the algorithm proposed in this work. The boundary have been chosen so that the results are independent of the way the boundary conditions are enforced. In the Su–Olson test case, the problem is symmetric. For the streaming test problem we use free boundary conditions as described in Eq. (37). For the transfer test case we use infinite opacities near the boundaries. The boundary conditions for the other test cases have been treated with a combination of such boundary conditions.

5.1. Su–Olson test case

This test case come from [32]. It is a basic non-equilibrium radiative transfer consisting of an initially cold, homogeneous, infinite, and isotropically scattering medium with an internal radiation source turned on at time zero [29].

The opacity is taken constant but with $C_v = \alpha T^3$. The source term $S = 1$ localized in $|x| \leqslant 1/2$. The system of equations to solve reduced to, see [29] for a precise derivation of the model,

$$\begin{aligned} &\partial_t E_r + \partial_x F_r = (T^4 - E_r) + S, \\ &\partial_t F_r + \partial_x P_r = -F_r, \\ &\partial_t T^4 = E_r - T^4. \end{aligned} \tag{42}$$

[2] Consider $Ax = b$ where $A = I - M$ and M is such that $m_{ij} \geqslant 0$ for $i \neq j$ and $\sum_i m_{ij} \leqslant 0$. The linear system is equivalent to $(1 - m_{ii})x_i = b_i + \sum_{j \neq i} m_{ij} x_j$. So $(1 - m_{ii})|x_i| \leqslant |b_i| + \sum_{j \neq i} m_{ij}|x_j|$. We get

$$\sum_i (1 - m_{ii})|x_i| \leqslant \sum_i |b_i| + \sum_i \sum_{j \neq i} m_{ij}|x_j| = \sum_i |b_i| + \sum_j (\sum_{i \neq j} m_{ij})|x_j|.$$

So $\sum_i |x_i| \leqslant \sum_i |b_i| + \sum_j (\sum_i m_{ij})|x_j| \leqslant \sum_i |b_i|$. The property is proved.

The problem is symmetric. The solution has not the time to reach the exterior boundary. This test problem has been used to benchmark various strategies about the analytical definition $(E_r, F_r) \mapsto P_r$, diffusion approximations, and numerical algorithms to solve the problem. In [29] it has been claimed that the variable Eddington factor gives non-smooth and oscillating solutions. On the contrary our results show that it is probably the numerical schemes used in [29] that were unstable for this test case, since our results are stable (i.e., non-oscillating) and accurate.

In Fig. 1, we plot the result given by scheme for the solution of (42) versus the solution of the diffusion approximation of the same model, that is

$$\partial_t E_r - \frac{1}{3}\partial_{xx} E_r = (T^4 - E_r) + S.$$

The solution of the diffusion approximation has been computed with a standard parabolic implicit finite difference scheme. For small time, we see a difference between diffusion and variable Eddington factor. For large time, both methods give the same result, as predicted by the theory. In all cases the solution of the variable Eddington model (42) is free of oscillations. It illustrates the stability and robustness of the algorithm proposed in this work. For large time the variable Eddington model admits theoretically the diffusion model as asymptotic limit. At the numerical level this is also true because $M_{j+\frac{1}{2}} = \frac{2}{2+\Delta x} \approx 1$ in the scheme, see Eq. (35).

In Fig. 2, we plot the Eddington factor $f = \frac{F_r}{E_r}$ at different times. The result is free of oscillations. One can compare with the results of [29, p. 629]. Moreover, $-1 \leqslant f \leqslant 1$ as stated in Proposition 7.

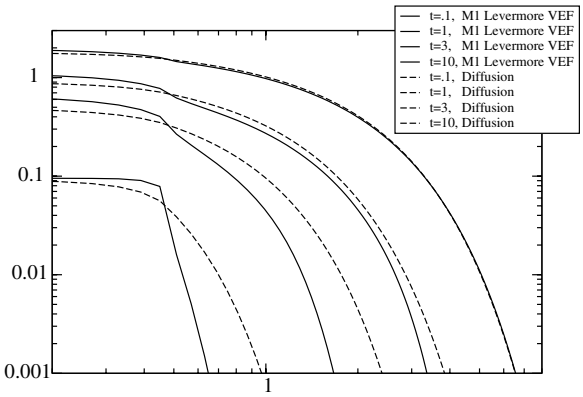

Fig. 1. Variable Eddington factor versus diffusion ($F_r = -\frac{1}{3}\partial_x E_r$) at different times. Radiative energy (log-scaled) versus the optical depth (log-scaled).

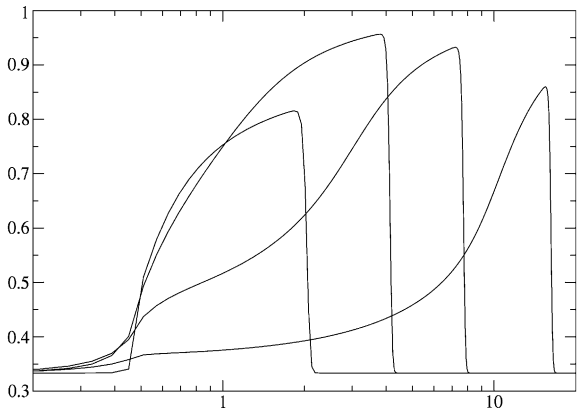

Fig. 2. Eddington factor $\chi(f)$ where $f = \frac{F_r}{E_r}$ versus the optical depth (log-scaled). Same times as in Fig. 1.

5.2. Streaming

This numerical test case illustrates the ability of the scheme to be accurate and stable for streaming. We solve (2) with $\sigma_a = \sigma_s = v = 0$ and $\varepsilon = 1$.

The initial data are

$$E_1 = F_r = \begin{cases} 1 & \text{if } 0.4 < x < 0.6, \\ 0 & \text{otherwise.} \end{cases}$$

We use free boundary conditions, standard for advection problems.

Since the velocity is one, the analytical solution at time $t = 0.2$ is

$$t = 0.2 : E_1 = F_r = \begin{cases} 1 & \text{if } 0.6 < x < 0.8, \\ 0 & \text{otherwise.} \end{cases}$$

The error in L^1 norm is given in Table 1. One sees that the scheme is of order 0.5 in L^1 norm. Since the scheme is implicit the price to pay is the extra numerical diffusion compared with an explicit discretization of the same model. However, an implicit scheme is absolutely needed for real applications where the velocity of light is very large. The numerical solution of Fig. 3 has been computed with the same code as for the Sue–Olson text case, with exactly the same scheme. The time step is $\Delta t = \frac{1}{2}\Delta x$.

5.3. Stationary case

We solve $\partial_t E_r + \frac{1}{\varepsilon}\partial_x F_r = \sigma_a(x)\frac{T^4 - E_r}{\varepsilon^2}$ and $\partial_t F_r + \frac{1}{\varepsilon}\partial_x P_r = -\sigma_t(x)\frac{F_r}{\varepsilon^2}$. The temperature T is prescribed $T = 1$ if $1.5 < x < 1.8$, $T = 0$ otherwise. The opacity σ_t is $\sigma_t = \bar{\sigma} = 1$ if $1 < x < 1.5$, $\sigma_t = 0$ otherwise. The opacity σ_a is $\sigma_a = 1$ if $1.5 < x < 2$, $\sigma_a = 0$ otherwise. The light's velocity is $\frac{1}{\varepsilon} = 10^3$. The boundary condition on the right is a prescribed source term with an infinite opacity. On the left it is a free boundary condition. Moreover, the support of the solution does not reach the right boundary.

For this problem it is possible to compute a quasi-analytical solution in the region $0 < x < 1.5$. For $x = 1.5$ one has a boundary condition $E_r = T_{1.5^+} = 1$. For $x < 1.5$ the stationary solution of the system is given by $\frac{1}{\varepsilon}\partial_x F_r = 0$ and $\frac{1}{\varepsilon}\partial_x P_r = -\sigma_t\frac{F_r}{\varepsilon^2}$. Therefore, F_r is constant $F_r \equiv F$. On the other hand, $P_r(1.5) - P_r(1) = -d\bar{\sigma}\frac{F}{\varepsilon}$,

Table 1
Error in L^1 norm for the streaming test case

Cells	100	200	400	800	1600
Error in L^1 norm	0.3	0.21	0.15	0.109	0.077

The order is approximatively 0.5.

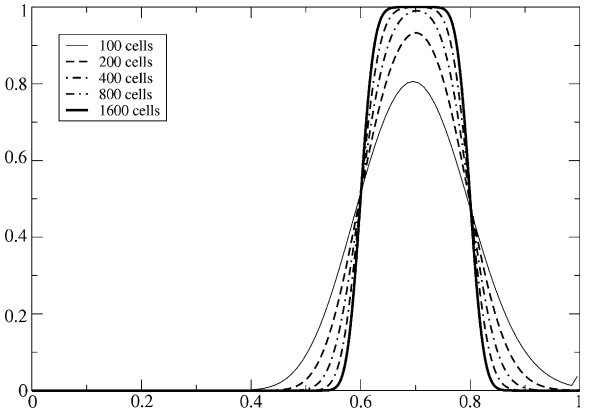

Fig. 3. Radiation energy versus x.

$d = 1.5 - 1$. Since $\sigma_a = 0$ for $x < 1$ the stationary regime is an outgoing regime with $F_r = -E_r$, $x < 1$. Therefore, $P_r(1.5) \approx \frac{E_r(1.5)}{3} = \frac{1}{3}$, $P_r(1) = E_r(1)$, $F = -E_r(1)$. Note that $P_r(1.5) \approx \frac{E_r(1.5)}{3}$ is a very accurate approximation because ε is small. Therefore, one solves for E_r and gets $E_r(1) = \frac{1}{3+3\bar{\sigma}d\varepsilon^{-1}} E_r(1.5) \approx 0$. In between $1 < x < 1.5$ one can solve for P_r which is affine with respect to x. Since $P_r \approx \frac{E_r}{3}$ is a very good approximation, then a quasi-analytical solution is

$$E_r(1) = 0, \quad E_r(1.5) = 1, \quad E_r \text{ is affine in between.} \tag{43}$$

We plot the result of our algorithm in Fig. 4. One sees a very good agreement between the numerical solution of Fig. 4 and the quasi-analytical solution (43).

5.4. Transfer

In this test case a transparent material is in between a hot opaque material on the left and a colder (but the temperature is non-zero) opaque material on the right. The physical solution is a radiative flow that comes from the left to the right, so that the right material becomes hotter and the left one becomes colder due to the conservativity of energy. We solve (22). The opacity σ_a is a function of the material and of the temperature

$$\sigma_a = \frac{\sigma_0}{T^3} \quad \text{with } \sigma_0 = \begin{cases} 0 & \text{for } 0.2 < x < 1.8, \\ 1 & \text{otherwise.} \end{cases}$$

The opacity σ_t does not play a important role in the simulation, and is here only to mimic totally opaque boundary conditions

$$\sigma_t = \begin{cases} 0 & \text{for } 0.1 < x < 1.9, \\ 10^4 & \text{otherwise.} \end{cases}$$

The initial data are $E_r \equiv 0$, $F_r \equiv 0$ and

$$T = \begin{cases} 1 & \text{for } 0.1 < x < 0.2, \\ 0 & \text{for } 0.2 < x < 1.8, \\ 0.1 & \text{for } 1.8 < x < 1.9. \end{cases}$$

The computation is done with 1000 cells. We use infinite opacities near the boundaries. The result is plotted in Fig. 5. As noticed in the legend of Fig. 5, the results are the same with the diffusion approximation. The reason is that for $t = 3$, which is quite a large time for this test problem, the radiative flux is almost zero in the transparent region. This is due to the multiple bounces of the radiative energy on both sides of the transparent region. To see a difference between the variable Eddington factor approach and the diffusion approximation, it is necessary to look at transitory regime around $x = 1.8$. This is done in Fig. 6 where we plot the history of temperature T (almost equal to the radiative temperature $T \approx T_r$ because the material is opaque) at $x = 1.8$ (in

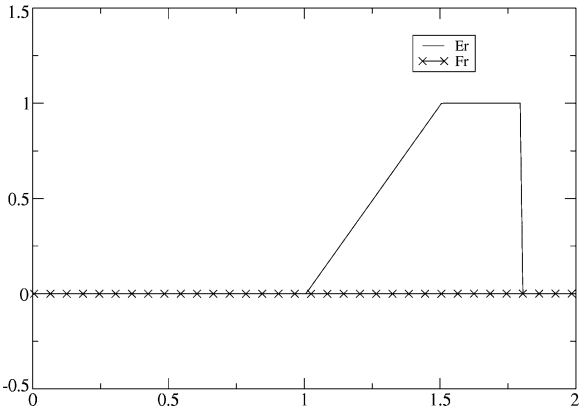

Fig. 4. Numerical solution for the stationary case. E_r and F_r versus x. The stationary source is for $x \geqslant 1.5$.

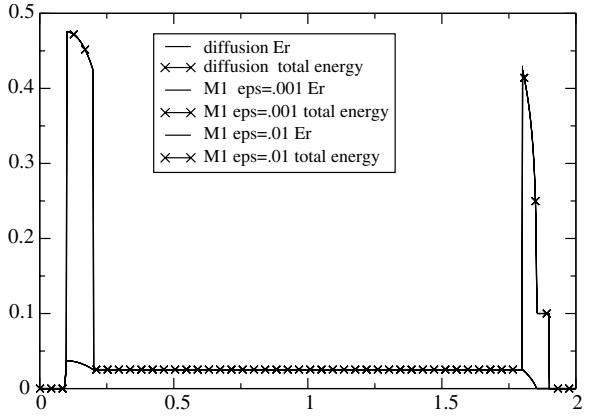

Fig. 5. $E_r = T_r^4$ and the total energy $T + E_r = T + T_r^4$ versus x at time $t = 3$, computed with the variable Eddington factor model and $\varepsilon = 10^{-3}$. For this test problem the result is the same with the diffusion approximation.

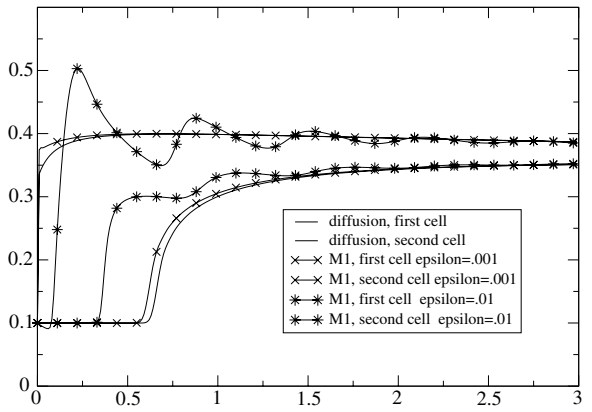

Fig. 6. Heating history in the opaque material: temperature T versus the time t for different models at $x = 1.8$ or $x = 1.84$.

the first opaque cell) and at $x = 1.84$ (in the opaque material). One sees a difference between the results depending on the model (which can be the diffusion approximation, the variable Eddington factor with $\varepsilon = 0.01$ and the variable Eddington factor with $\varepsilon = 0.001$) and on the point ($x = 1.8$ or $x = 1.84$). Essentially the variable Eddington factor with $\varepsilon = 0.001$ is very close to the diffusion approximation. However, the variable Eddington factor with $\varepsilon = 0.01$ is slightly different. Oscillations have appeared that we interpret as the result of multiple radiative bounces between the opaque materials. For longer time, all models have the same history.

5.5. Coupling with hydrodynamics

5.5.1. Radiative Riemann problem

If now we set $\sigma_a = 0$ and $\sigma_s = +\infty$ then we obtain the simplified hyperbolic set of equations

$$\begin{aligned}
&\frac{\partial}{\partial t}(\rho) + \frac{\partial}{\partial x}(\rho v) = 0,\\
&\frac{\partial}{\partial t}(\rho v) + \frac{\partial}{\partial x}(\rho v^2 + p + p_r) = 0, \quad p_r = \frac{E_r}{3},\\
&\frac{\partial}{\partial t}(\rho E + E_r) + \frac{\partial}{\partial x}(\rho E v + p v + p_r v) = 0, \quad E_r = T_r^4,\\
&\frac{\partial}{\partial t} S_r + \frac{\partial}{\partial x}(u S_r) = 0, \quad S_r = T_r^3.
\end{aligned} \tag{44}$$

For this system we study a standard Riemann problem. The initial data are $\rho = 1$, $u = 0$, $p = 1$, $T_r = 1$ for $x < 0.5$, and $\rho = 0.125$, $u = 0$, $p = 0.1$, $T_r = 0.1$ for $x > 0.5$. The solution consists in a rarefaction fan, a contact discontinuity and a shock. Across the shock and the rarefaction fan $\frac{T_r^3}{\rho}$ is preserved. A lot of hydrodynamic solvers can be used for the numerical resolution. We have used a standard Lagrange + remap solver with an acoustic flux. We use standard free boundary conditions well adapted for pure hyperbolic problems.

The results, which are exactly the same for the diffusion approximation and the variable Eddington factor model, are displayed in Fig. 7 for the density, velocity and total pressure, and in 8 for $\frac{T_r^3}{\rho} = \frac{S_r}{\rho}$, see [35,1].

5.5.2. Radiation hydrodynamics

For this test problem we solve the full radiation hydrodynamics (20) (using the splitting scheme (21) and (22)) and with the variable Eddington factor given in (2). The initial data are

$$\begin{aligned}
&x < 0.4 \text{ and } x > 1.6 : \rho = 0.1, \quad u = 0, \quad p_{\text{hydro}} = 0.002, \quad T_r = T = \varepsilon/cv, \quad F_r = 0,\\
&0.4 < x < 0.8 \text{ and } 1.2 < x < 1.6 \} \ \rho = 0.01, \quad u = 0, \quad p_{\text{hydro}} = 0.0002, \quad T_r = T = \varepsilon/cv, \quad F_r = 0,\\
&0.8 < x \text{ and } x < 1.2 : \rho = 0.1, \quad u = 0, \quad p_{\text{hydro}} = 0.001, \quad T_r = 1, \quad F_r = 0.
\end{aligned}$$

The opacities are

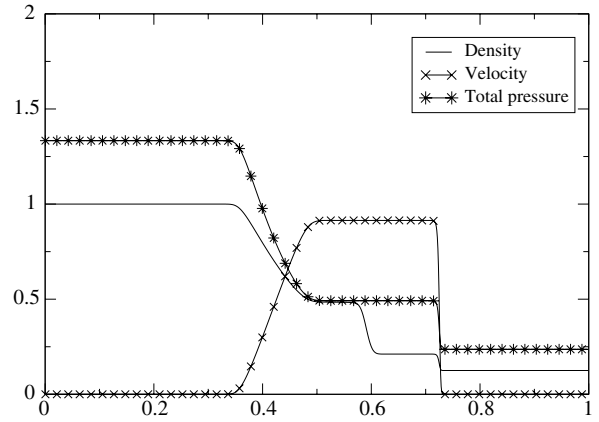

Fig. 7. Density, velocity and total pressure versus the position x at $t = 0.1$ with 1000 cells: CFL = 0.5.

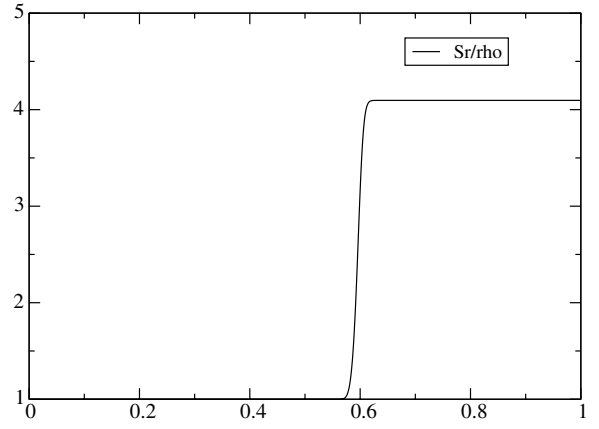

Fig. 8. Radiative entropy $\frac{T_r^3}{\rho} = \frac{S_r}{\rho}$ versus x at $t = 0.1$ with 1000 cells: CFL = 0.5. One notices the exact preservation of this quantity across the shock and the rarefaction fan.

$$\sigma \equiv 0, \quad \tau = \begin{cases} 0.2 & \text{in the left, central and right regions,} \\ 0.2 \times 10^{-7} & \text{otherwise.} \end{cases}$$

An energy deposit is made at each time step in the central region

$$\varepsilon \Leftarrow \varepsilon + 50000 \times \Delta t.$$

Since the central region is hotter, then a flow a radiative energy passes through the transparent intermediate regions, and arrived at the borders of the opaque extreme two regions. The time of observation is such that the solution has not reach the exterior boundaries.

A zoom around $x = 0.4$ is given in Fig. 9. One sees that diffusion is in advance with respect to the variable Eddington factor. An interpretation is that diffusion propagates instantaneously the radiation since the equation is global. Therefore, the radiation is over-predicted with the diffusion model. On the other hand, the variable Eddington factor is an hyperbolic model with finite speed of propagation. The radiation takes some time to arrive in the region, coming from the central region. Our results are stable.

We give a global view of the radiative quantities, E_r, F_r and $f = \frac{F_r}{E_r}$ in Fig. 10. The result is limited since $|f| \leqslant 1$ everywhere. In Fig. 11, we plot the the radiative energy E_r in the interval $0 < x < 1$ for 100 and 400 cells, to illustrate the stability and convergence of the diffusion approximation and the variable Eddington factor method. Both schemes are equally stable. The diffusion gives a flat profile due to the infinite propagation speed of this model.

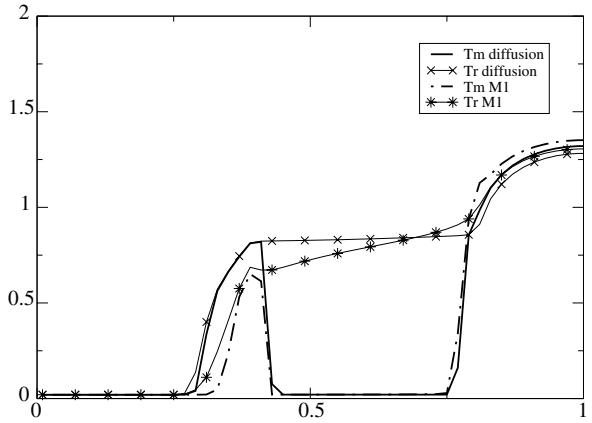

Fig. 9. T and T_r versus the position x for diffusion and the variable Eddington factor, 100 cells, $T = 0.005$.

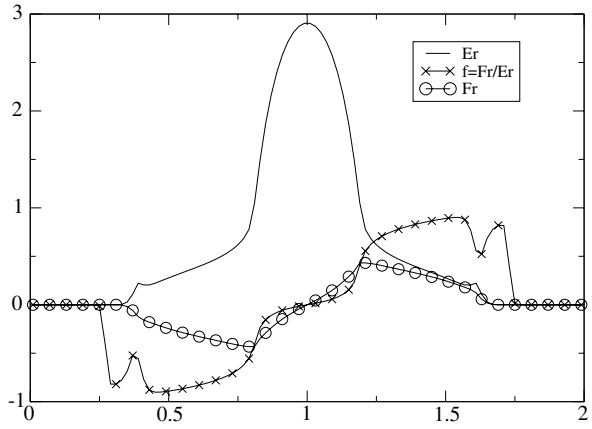

Fig. 10. E_r, F_r and $f = \frac{F_r}{E_r}$ versus the position x: 100 cells, $T = 0.005$.

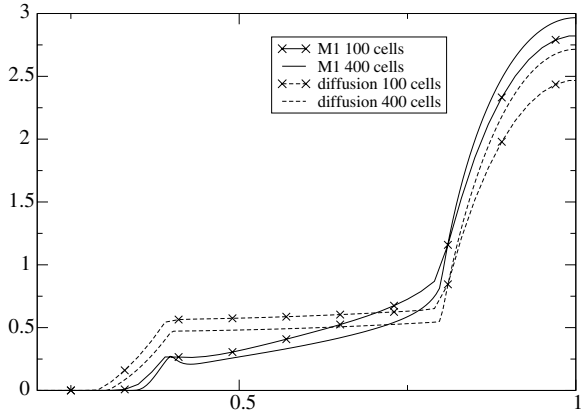

Fig. 11. Convergence study of the radiative energy plotted versus the position x: 100 and 400 cells.

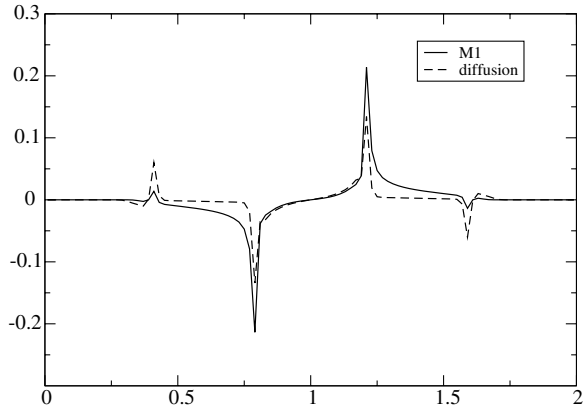

Fig. 12. Material velocity u versus the position x at a given time.

In Fig. 12, we plot the velocity obtained with the diffusion approximation and with the variable Eddington factor method. The physics of the problem is the following: an energy deposit his made by the radiation at the interface opaque/transparent $x = 0.4$. Therefore, the pressure increases and pushes the opaque material on the left ($u < 0$ for $x < 0.4$) and the transparent material on the right ($u > 0$ for $0.4 < x < 0.4 + \varepsilon$). Nevertheless

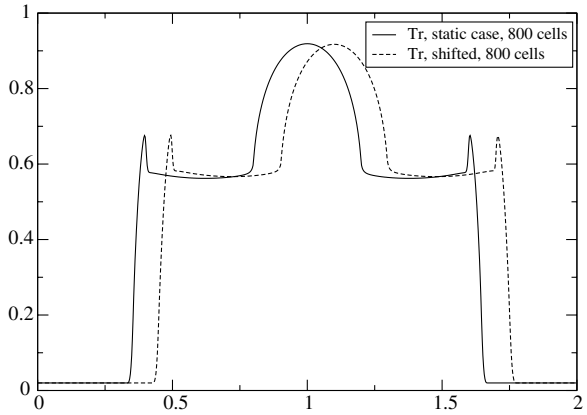

Fig. 13. Shifted versus non-shifted calculations. E_r versus x.

there are some differences. Essentially the velocity profile is flat and equal to 0 for $0.5 < x < 0.8$ computed with the diffusion approximation. A possible interpretation is the infinite speed of propagation of the diffusion approximation which enforces a constant pressure (therefore no acceleration in this region). On the other hand, the propagation of speed is finite with the variable Eddington factor method : it explains the smooth acceleration on the left of the material in the region $0.5 < x < 0.8$. However, the time scale is the time scale of radiation, which is much smaller than the hydrodynamics time scale. So the impact of these velocity fields is absolutely negligible on the density.

In the final test case, Fig. 13, we have zeroed the energy deposit. The velocity is $v = 0$ and $v = 200$, everywhere at time $t = 0$. Therefore, we expect the solution with $v = 200$ to be equal to the solution with $v = 0$, but with a shift. The results show it is indeed the case. For this particular test problem, we found necessary to advect the opacity with an *exact* method. If not numerical diffusion smear the opacity profiles at the interfaces opaque/transparent which give bad results. Here the results are good.

6. Conclusion and perspectives

We think that the method proposed in this work gives good results in 1D. At least the method is stable and accurate for diffusion limits, the code is robust, and the numerical results are satisfactory for a large variety of test cases. One could also think about coupling the scheme proposed in this work with higher order schemes with a θ-method. The interest could be a less dissipative scheme in free streaming regions.

The method does not depend on the particular Eddington factor used for radiation, and therefore can be used in other areas, for neutrinos [31], electrons and all models with the same structure where the diffusion limit is somehow the isotropization of a more general system of partial differential equations [4].

Currently, we work on the extension for multidimensional problems. The interest of moment models for multidimensional problems could be a better treatment of the anisotropy of radiation.

References

[1] C. Buet, B. Despres, Asymptotic analysis of fluid models for the coupling of radiation and hydrodynamics, J. Quant. Spectrosc. Radiat. Transfer 85 (3–4) (2004) 385–418.
[2] E. Audit, P. Charrier, J.-P. Chieze, B. Dubroca, A radiation-hydrodynamics scheme valid from the transport to the diffusion limit, 2002. Available from: <lanl.arxiv.org/abs/astro-ph/0206281>.
[3] A. Berman, R.J. Plemmons, Non Negative Matrices in the Mathematical Sciences, Classics in Applied Mathematics, SIAM, Philadelphia, PA, 1994.
[4] F. Bouchut, Nonlinear stability of finite volume methods for hyperbolic conservation laws, and well-balanced schemes for sources Frontiers in Mathematics Series, Birkhaüser, Basel, 2004.
[5] T.A. Brunner, J.P. Holloway, One-dimensional Riemann solvers and the maximum entropy closure, JQRST 69 (2001) 543–566.
[6] C. Buet, S. Cordier, Asymptotic preserving scheme and numerical methods for radiative hydrodynamic models, Comp. R. Math. 338 (12) (2004) 951–956.
[7] C. Buet, S. Cordier, An asymptotic preserving scheme for hydrodynamics radiative transfer models, Numer. Math. (submitted).
[8] F. Coquel, C. Marmignon, Numerical methods for weakly ionized gas, Astrophys. Space Sci. 260 (1–2) (1998) 15–27.
[9] W. Wenlong Dai, Paul R. Woodward, Numerical simulations for radiation hydrodynamics: II. Transport limit, J. Comput. Phys. 157 (1) (2000) 199–233.
[10] J.L. Feugeas, B. Dubroca, Entropy moment closure hierarchy for the radiative transfer equation, C. R. Acad. Sci., Paris, Sér. I, Math. 329 (10) (1999) 915–920.
[11] L. Gosse, Localization effects and measure source terms in numerical schemes for Balance laws, Math. Comp. 71 (238) (2002) 553–582.
[12] L. Gosse, G. Toscani, Space localization and well-balanced schemes for discrete kinetic models in diffusive regime, SIAM J. Numer. Anal. 41 (2003) No. 2641-658.
[13] L. Gosse, A well-balanced scheme using non-conservative products designed for hyperbolic systems of conservation laws with source terms, Math. Mod. Meth. Appl. Sci. 11 (2001) 339–365.
[14] S. Jin, C.D. Levermore, Numerical schemes for hyperbolic conservation laws with stiff relaxation terms, J. Comput. Phys. 126 (1996) 449–467. Article No.0149.
[15] S. Jin, L. Pareschi, G. Toscani, Uniformly accurate diffusive relaxation schemes for multiscale transport equations, SIAM J. Numer. Anal. 38 (2000) 913.
[16] S. Jin, Z. Xin, The relaxation schemes for systems of conservation laws in arbitrary space dimensions, Commun. Pure Appl. Math. 48 (1995) 235–276.
[17] T.Y. Hou, P.G. LeFloch, Why nonconservative schemes converge to wrong solutions: error analysis, Math. Comput. 62 (1994) 497–530.

[18] C.D. Levermore, Relating Eddington factors to flux limiters, J. Quant. Spectrosc. Radiat. Transfer 31 (2) (1984) 149–160.
[19] C.D. Levermore, Moment closure hierarchies for kinetic theories, J. Stat. Phys. 83 (5–6) (1996) 1021–1065.
[20] R.B. Lowrie, J.E. Morel, J.A. Hittinger, The coupling of radiation and hydrodynamics, Astrophys. J. 521 (1999) 432–450.
[21] R.B. Lowrie, J.E. Morel, Issues with high-resolution Godunov methods for radiation hydrodynamics, J. Quant. Spectrosc. Radiat. Transfer 69 (4) (2001) 475–489.
[22] R.B. Lowrie, J.E. Morel, Discontinuous Galerkin for hyperbolic systems with sti relaxation, in: B. Cockburn, G.E. Karniadakis, C.W. Shu (Eds.), Discontinuous Galerkin Methods: Theory, Computation and Applications, Springer, Berlin, 2000, p. 385.
[23] R.B. Lowrie, J.E. Morel, Methods for hyperbolic systems with stiff relaxation, Int. J. Numer. Meth. Fluids 40 (2002) 413–423.
[24] D. Mihalas, Computational Methods for Astrophysical Fluid Flow, Saas-Fee Advandced Course, Lectures Notes, Springer, Berlin, 1997.
[25] D. Mihalas, B.W. Mihalas, Foundations of Radiation Hydrodynamics, Oxford University Press, Oxford, 1984.
[26] G.N. Minerbo, Maximum entropy Eddington factors, J. Quant. Spectrosc. Radiat. Transfer 20 (1978) 541–545.
[27] I. Müller, T. Ruggeri, Rational Extended Thermodynamics, second ed.Springer Tracts in Natural Philosophy, vol. 37, Springer, New York, NY, 1999.
[28] G. Naldi, L. Pareschi, Numerical schemes for hyperbolic systems of conservation law with stiff diffusive relaxation, SIAM J. Numer. Anal. 37 (4) (2000) 1246–1270.
[29] G. L, Olson, L.H. Auer, M.L. Hall, Diffusion, P^1, and other approximate forms of radiation transport, Los Alamos Report LA-UR-99-471.
[30] Y. Saillard, Hydrodynamique de l'implosion d'une cible FCI, Comptes Rendus de l'Académie des Sciences – Series IV – Physics, vol. 1 (6), August, 2000, pp. 705–718.
[31] J.M. Smit, J. Cernohorsky, C.P. Dullemond, Hyperbolicity and critical points in two-moments approximate radiative transfer, Astron. Astrophys. 325 (1997) 203–211.
[32] B. Su, G.L. Olson, Ann. Nucl. Energy 24 (1997) 1035–1055.
[33] A.I. Shestakov, J.A. Greenough, L.H. Howell, Solving the radiation diffusion and energy balance equations using pseudo-transient continuation, J. Quant. Spectrosc. Radiat. Transfer 90 (2005).
[34] E.F. Toro, Riemann Solvers and Numerical Methods for Fluid Dynamics: A Practical Introduction, Springer, Berlin, 1997.
[35] Ya.B. Zel'dovich, Yuri P. Raizer, Physics of Shock Waves and High-Temperature Hydrodynamic Phenomena, Dover Publications, New York, 2002.